

# Spatial Autoregressive Models for Ecological Inference

Jay M. Ver Hoef<sup>1</sup>, Erin E. Peterson<sup>2</sup>, Mevin B. Hooten<sup>3</sup>, Ephraim M. Hanks<sup>4</sup>, and Marie-Josée Fortin<sup>5</sup>

---

<sup>1</sup>National Marine Mammal Laboratory, NOAA-NMFS Alaska Fisheries Science Center  
7600 Sand Point Way NE, Seattle, WA 98115  
tel: (907) 456-1995      E-mail: jay.verhoef@noaa.gov

<sup>2</sup> ARC Centre for Excellence in Mathematical and Statistical Frontiers (ACEMS) and  
the Institute for Future Environments, Queensland University of Technology

<sup>3</sup> U.S. Geological Survey, Colorado Cooperative Fish and Wildlife Research Unit,  
Department of Fish, Wildlife, and Conservation Biology  
Department of Statistics, Colorado State University

<sup>4</sup> Department of Statistics, Penn State University

<sup>5</sup> Department of Ecology and Evolutionary Biology, University of Toronto

---

March 1, 2016

## Summary

1. We review conditional autoregressive (CAR) and simultaneous autoregressive (SAR) models for spatial ecological data because they are under-used, or used incorrectly, and this is likely because they are more difficult to understand than geostatistical models. To highlight their usefulness, we identify and discuss six ecological inferences using CAR and SAR models, including model selection, spatial regression, estimation of autocorrelation, estimation of other connectivity parameters, spatial prediction, and spatial smoothing.
2. We compare and contrast CAR and SAR models, showing their development and connection to partial correlations. Special cases, such as the intrinsic autoregressive model (IAR), are also shown. Practical use of CAR and SAR models depends on weight matrices, and neighborhood definition and row-standardization are important concepts when developing such matrices. Weight matrices can also include ecological covariates and connectivity structures, which we encourage but have been rarely used.
3. Trends in harbor seals (*Phoca vitulina*) in southeastern Alaska from 463 polygons, some with missing data, are used to illustrate the six ecological inferences and highlight discussion points from the earlier review. We develop a variety of weight matrices, and CAR and SAR models are fit to data using maximum likelihood and Bayesian methods. We compare models and present spatial regression results for several models. Profile likelihood graphs illustrate inference for covariance parameters. The same data set is used for both prediction and smoothing, and the relative merits of each are discussed. We show the nonstationary variances and correlations of a CAR model and demonstrate the effect of row-standardization.
4. We recommend that ecologists make greater use of autoregressive models, both directly and in hierarchical models, and not only in explicit spatial settings, but also for more general connectivity and graphical models. We conclude with some take-home lessons for CAR and SAR models, including 1) thoughts on choosing between CAR and IAR models, 2) modeling ecological effects in the covariance matrix, 3) the appeal of spatial smoothing, 4) how to handle isolated neighbors, and 5) software considerations.

31

---

32

33 KEY WORDS: Conditional autoregressive, simultaneous autoregressive, CAR, SAR, IAR, geostatis-  
34 tics, prediction, smoothing

35

## INTRODUCTION

When data are collected at spatial locations, Cressie (1993, p. 8) divides spatial statistical models into two broad classes: 1) point-referenced geostatistical models, and 2) lattice models, also called areal models (Banerjee et al., 2004). The two most common lattice models are the conditional autoregressive (CAR) and simultaneous autoregressive (SAR) models. The defining characteristic for CAR and SAR models is that the data occur on a (possibly irregular) grid, or lattice, with a countable set of nodes. Geostatistical models, on the other hand, are used for data that are spatially continuous (a continuous surface). Another distinction that we find more useful for conceptual understanding is that geostatistical models use spatial information to directly model a covariance matrix, whereas CAR and SAR models use spatial information to model the inverse of a covariance matrix (also known as the precision matrix). Modeling the precision matrix is less intuitive than modeling the covariance matrix, which may make it more difficult to understand the implications of modeling decisions. Indeed, in certain circumstances Wall (2004) found some surprising and unusual behavior for CAR and SAR models. The less intuitive precision matrix, and a reputation for unusual behavior, may unfortunately keep some scientists from using these models, or using them incorrectly. For example, papers have incorrectly compared CAR/SAR to geostatistical models (e.g., Beguería and Pueyo, 2009), incorrectly formulated the CAR model (e.g., Keitt et al., 2002), and have given incorrect relationships between CAR and SAR models (e.g., Dormann et al., 2007). We do not dwell on these (details are given in Appendix A), but rather they illustrate that good statistical practice with CAR and SAR models depends on more and better information. CAR and SAR models have many useful applications (e.g., Gelfand et al., 2005; Latimer et al., 2006; Magoun et al., 2007; Hanks and Hooten, 2013). Our objective is to review CAR and SAR models in a practical way, so that their potential may be more fully realized and used by ecologists.

First we motivate the uses of spatial autoregressive models with typical (and not so typical, but useful) objectives for ecological studies (Table 1). For objective 1, model selection, there are a plethora of model comparison methods, or multimodel inferences, based on AIC, BIC, etc., that are available (see, e.g., Burnham and Anderson, 2002). CAR and SAR covariance matrices may be part

of some or all models, and choosing a model, or comparing various CAR and SAR models, may be an  
important goal of the investigation. For objective 2, regression, an early and influential paper on using  
CAR models for Scottish lip cancer data (Clayton and Kaldor, 1987) found that the covariate “%  
agriculture” helped explain lip cancer rates among counties in Scotland, in conjunction with a CAR  
model for spatial autocorrelation. For another example, in a spatial CAR regression model using  
wolverine data (Gardner et al., 2010), the probability of occupancy depended on covariates related  
to elevation and human influence in the plots. As an example for objective 3, autocorrelation, using  
a Bayesian model, Gardner et al. (2010) provide estimates of an autocorrelation parameter, along  
with credibility intervals. Objective 4, covariate effects on autocorrelation, is almost never used in  
ecological models, or in other disciplines, but we give an example later. Generally, the neighborhood  
structure that forms the covariance matrix is considered a nuisance; that is, it is a requirement to  
acknowledge spatial autocorrelation to make valid inferences on the other objectives in this list. An  
example of objective 5, prediction, for CAR models is given in Gardner et al. (2010), who modeled  
occupancy of wolverines from aerial surveys, and there were three types of observations: 1) plots  
that were surveyed with observed animals, 2) plots that were surveyed with no animals, and 3)  
unsurveyed plots. Predictions for unsurveyed plots provided probabilities of wolverine occurrence.  
Objective 6, smoothing, is the classic idea behind the Scottish lip cancer data (Clayton and Kaldor,  
1987). In this example, all counties have observed cancer rates. To conceptualize the smoothing  
objective, imagine that disease rates in administrative districts are generally low, say less than  
10% based on thousands of samples, but spatially patterned with areas of lower and higher rates.  
However, one administrative district has a single sample that is positive for the disease. It would be  
unrealistic to estimate the whole administrative district to have 100% disease rates based on that  
single sample. The models of Clayton and Kaldor (1987) create rates that smooth over observed  
data by using values from nearby locations to provide better estimates, in general.

Based on the introduction above, it should be clear that CAR and SAR models can be used  
in many applications for ecological data. Our objectives are: 1) to explain, in ecological terms, how  
these models are obtained, 2) give insight and intuition on how they work, 3) to compare CAR  
and SAR models, and 4) give practical guidelines for their use. We provide an example for further

illustration of the objectives given in Table 1. For discussion, identify areas that have received little attention so far. For example, there is little guidance in the literature on handling isolated (unconnected) sites, or how to choose between a CAR model and a special case of the CAR model, the intrinsic autoregressive model (IAR). We provide such guidance, and finish with five take-home messages that deserve more attention.

## SPATIAL AUTOREGRESSIVE MODELS

Spatial autocorrelation, or autocovariance, quantitatively represents the degree of statistical dependency between random variables using spatial relationships (Cressie, 1993). It is a common characteristic of ecological data, which are often collected at a specific location in space and in time. Analyzing spatially correlated data requires the use of spatial statistical models because the assumption of independence is violated, making many conventional statistical methods inappropriate.

In general terms, a spatial statistical model accounts for the spatial location of the data (i.e., spatial indexing) in the probabilistic part of the model. A wide variety of methods have been developed and so it is useful to start with a general representation of a spatial statistical model,  $\{Z(\mathbf{s}) : \mathbf{s} \in D\}$  (Cressie, 1993, pg. 8). Here,  $Z$  is an observed or unobserved random variable at location  $\mathbf{s}$ , which belongs to the spatial domain of interest  $D$ . The random variable could represent the presence or absence of a species, percent canopy cover, allele counts, etc., while the domain of interest could be a study area, a management unit, or a biogeographic region, etc. In this paper we focus on spatial models where  $D$  is a finite set and where distance is not necessarily uniquely defined. For example, political administrative districts (such as counties, boroughs, etc.) have area, any set of them is a finite number; they are spatially well-defined, generally as a polygon in a computer system such as a geographic information system (GIS), but (Euclidean) distance between areal units is not well-defined because that requires two points in a Euclidean coordinate system. Rather than model spatial autocovariance based on Euclidean distance, as is common in geostatistics, spatial relationships for areal data are based on a graphical model, or a network,

where sites are depicted as nodes, and edges denote connections. Edges can be defined in many ways, but a common approach is to create an edge between adjoining administrative units.

The covariance matrices of geostatistical models, where  $\mathbf{s}$  varies continuously within  $D$ , could be used directly to model data from a finite set of locations within  $D$  if Euclidean distance was an appropriate way to express their correlation. The main problem with geostatistical models is that they are guaranteed to be valid only for Euclidean metrics. Consider the case where binary values are used to express connections; the resulting topology is no longer guaranteed to be a Euclidean space. For example, Ver Hoef et al. (2006) show how nodes, connected in a branching network (representing stream nodes), create a topology for which covariance matrices from commonly-used geostatistical models are inappropriate. In this case, one possibility is to create models that are appropriate for the topology (e.g., Ver Hoef and Peterson, 2010), but stream networks are a special topology, and such models are not general. Alternatively, the topology could be deformed to match Euclidean space, such as is done in multidimensional scaling (Curriero, 2006), but this suffers from sensitivity to the exact configuration of points. That is, adding or dropping a node changes the multidimensional scaling. There is a class of statistical models, however, that are ready-made for spatial network models; the spatial autoregressive models. As we demonstrate, these models are specified through the inverse of the covariance matrix, so they are somewhat less intuitive. For that reason, we now discuss them and attempt to give a fuller understanding of their properties.

Spatial autoregressive models are, fundamentally, not spatial at all. They are also known as graphical models (e.g., Lauritzen, 1996; Whittaker, 2009) and Gaussian Markov random fields (e.g., Rue and Held, 2005). However, when spatial information is used to define nodes and edges, they are also known as lattice models (e.g., Cressie, 1993, pg. 8) or areal models (e.g., Banerjee et al., 2004, pg. 69). These models differ from the geostatistical models because  $D$  is fixed and finite, rather than continuous (Cressie, 1993, pg. 8). As mentioned previously, an areal unit may not have a single set of spatial coordinates and so the data are indexed by  $i$  in the graphical model, rather than  $\mathbf{s}$ . For example,  $Z_i$  is the random variable for the  $i$ th node, where  $i = 1, 2, \dots, N$ . Now

143 consider the spatial regression framework,

$$\mathbf{y} = \mathbf{X}\boldsymbol{\beta} + \mathbf{z} + \boldsymbol{\varepsilon}, \quad \text{eqn 1}$$

144 where the goal is to model a first-order mean structure that includes covariates (i.e., predictor  
 145 variables,  $\mathbf{X}$ , measured on nodes), as well as a latent spatial random process  $\mathbf{z}$ , where  $\mathbf{z} \sim \mathcal{N}(\mathbf{0}, \boldsymbol{\Sigma})$ ,  
 146 and independent error  $\boldsymbol{\varepsilon}$ , where  $\boldsymbol{\varepsilon} \sim \mathcal{N}(\mathbf{0}, \sigma_{\varepsilon}^2 \mathbf{I})$ . Note that  $\mathbf{z}$  is not directly measured, and instead  
 147 must be inferred using a statistical model. The spatial regression framework becomes a spatial  
 148 autoregressive model when the covariance matrix,  $\boldsymbol{\Sigma}$ , takes one of two main forms: 1) the SAR  
 149 model,

$$\boldsymbol{\Sigma} \equiv \sigma_Z^2 ((\mathbf{I} - \mathbf{B})(\mathbf{I} - \mathbf{B}')^{-1}), \quad \text{eqn 2}$$

150 or, 2) the CAR model,

$$\boldsymbol{\Sigma} \equiv \sigma_Z^2 (\mathbf{I} - \mathbf{C})^{-1} \mathbf{M}. \quad \text{eqn 3}$$

151 Here, spatial dependency between  $Z_i$  and  $Z_j$  is modeled by  $\mathbf{B} = \{b_{ij}\}$  and  $\mathbf{C} = \{c_{ij}\}$  for the  
 152 SAR and CAR models, respectively, where  $b_{ii} = 0$  and  $c_{ii} = 0$  and  $\mathbf{M} = \{m_{ij}\}$  is a diagonal  
 153 matrix ( $m_{ij} = 0 \ \forall \ i \neq j$ ), where  $m_{ii}$  is proportional to the conditional variance of  $Z_i$  given all  
 154 of its neighbors. The spatial dependence matrices can be further decomposed into  $\mathbf{B} = \rho \mathbf{W}$  and  
 155  $\mathbf{C} = \rho \mathbf{W}$ , where  $\mathbf{W}$  is a weights matrix and  $\rho$  controls the strength of dependency.

156 To help understand autoregressive models, consider partial correlation (e.g., Snedecor and  
 157 Cochran, 1980, pg. 361), which is the idea of correlation between two variables after “controlling,”  
 158 or holding fixed, the values for all others variables. If  $\boldsymbol{\Sigma}^{-1} = \boldsymbol{\Omega} = \{\omega_{i,j}\}$ , then the partial correlation  
 159 between random variable  $Z_i$  and  $Z_j$  is  $-\omega_{ij} / \sqrt{\omega_{ii}\omega_{jj}}$  (Lauritzen, 1996, pg. 120), which, for normally  
 160 distributed data, is equivalent to conditional dependence. Thus, we can see that the CAR model, in  
 161 particular, allows the modeler to directly specify partial correlations (or covariances), rather than  
 162 correlation directly. That is, we are in control of specifying the off-diagonal matrix values of  $\mathbf{W}$  in  
 163  $\boldsymbol{\Sigma}^{-1} = \sigma_Z^2 \mathbf{M}^{-1} (\mathbf{I} - \rho \mathbf{W})$ , and therefore we are specifying the partial correlations. The SAR model  
 164 case is similar, though instead of directly specifying partial correlations, as is done with  $(\mathbf{I} - \mathbf{C})$  in



the CAR model, the SAR specification involves modeling a square root,  $(\mathbf{I} - \mathbf{B})$ , of the precision matrix, which encodes partial correlations. Contrast this to geostatistics, where we are in control of specifying  $\mathbf{\Sigma}$ , and therefore we are specifying the correlations. In both cases, we generally use some algorithm, often with parameters, rather than specifying every matrix entry individually. For CAR and SAR models, the algorithm is often based on neighbors (e.g., partial correlation exists between neighbors that share a boundary), and for geostatistics the algorithm is based on distance (e.g., correlation depends on an exponential decay with distance). If  $b_{ij} = 0$  or  $c_{ij} = 0$ , they are partially uncorrelated; otherwise there is partial dependence. Note that  $b_{ii}$  and  $c_{ii}$  are always zero. In order for  $\mathbf{z}$  (a SAR or CAR random variable) to have a proper statistical distribution,  $\rho$  must lie in a range of values that allows  $(\mathbf{I} - \mathbf{B})(\mathbf{I} - \mathbf{B}')$  or  $(\mathbf{I} - \mathbf{C})$  to have an inverse; that is,  $\rho$  cannot be chosen arbitrarily, and its range depends on the weights in  $\mathbf{W}$ .

The statistical similarities among the SAR and CAR models are obvious; they both rely on a latent Gaussian specification, a weights matrix, and a correlation parameter. In that sense, both the SAR and CAR models can be implemented similarly. However, there are key differences between SAR and CAR models that are fundamentally important because they impact the inferences that are gained from these models. As such, we describe each model in more detail, and later we give more practical advice.

## SAR Models

One approach for building the SAR model begins with the usual regression formulation described in (eqn 1). Now, instead of modeling the correlation of  $\mathbf{z}$  directly, an explicit autocorrelation structure is imposed,

$$\mathbf{z} = \mathbf{B}\mathbf{z} + \boldsymbol{\nu}, \tag{eqn 4}$$

where the spatial dependence matrix,  $\mathbf{B} = \rho\mathbf{W}$ , is relating  $\mathbf{z}$  to itself, and  $\boldsymbol{\nu} \sim N(\mathbf{0}, \sigma_z^2\mathbf{I})$ . These models are generally attributed to Whittle (1954). Solving for  $\mathbf{z}$ , note that  $(\mathbf{I} - \mathbf{B})^{-1}$  must exist (Cressie, 1993; Waller and Gotway, 2004), and then  $\mathbf{z}$  has zero mean and covariance matrix  $\sigma_z^2((\mathbf{I} - \mathbf{B})(\mathbf{I} - \mathbf{B}'))^{-1}$ . The spatial dependency in the SAR model comes from the matrix  $\mathbf{B}$  that causes the

simultaneous autoregression of each random variable on its neighbors. When constructing  $\mathbf{B} = \rho\mathbf{W}$ , the weights matrix  $\mathbf{W}$  does not have to be symmetric because it does not appear directly in the inverse of the covariance matrix (i.e., precision matrix). However, there are obvious constraints to allow  $(\mathbf{I} - \mathbf{B})(\mathbf{I} - \mathbf{B}')$  to be a precision matrix.. These constraints are best explored through the eigenvectors and eigenvalues of  $\mathbf{W}$ . The matrix  $\mathbf{W}$  must be nonsingular; that is, it cannot have any zero eigenvalues. Also, if  $\lambda_{[1]} < 0$  is the smallest eigenvalue, and  $\lambda_{[N]} > 0$  is the largest eigenvalue of  $\mathbf{W}$ , then  $1/\lambda_{[1]} < \rho < 1/\lambda_{[N]}$ .

The model created by (eqn 1) and (eqn 4) has been termed the “error” model version of SAR models. An alternative is to simultaneously autoregress the whole response variable, not just the errors,  $\mathbf{y} = \rho\mathbf{W}\mathbf{y} + \mathbf{X}\boldsymbol{\beta} + \boldsymbol{\varepsilon}$  (Anselin, 1988), yielding

$$\mathbf{y} = (\mathbf{I} - \rho\mathbf{W})^{-1}\mathbf{X}\boldsymbol{\beta} + (\mathbf{I} - \rho\mathbf{W})^{-1}\boldsymbol{\varepsilon}, \quad \text{eqn 5}$$

which allows the matrix  $\mathbf{W}$  to smooth covariates in  $\mathbf{X}$  as well as creating autocorrelation in the error for  $\mathbf{y}$ . A final version is to simultaneously autoregress both response and a separate random effect  $\boldsymbol{\nu}$ ,

$$\mathbf{y} = \rho\mathbf{W}\mathbf{y} + \mathbf{X}\boldsymbol{\beta} + \mathbf{W}\mathbf{X}\boldsymbol{\nu} + \boldsymbol{\varepsilon}, \quad \text{eqn 6}$$

see, e.g., Kissling and Carl (2008).

## CAR Models

The term “conditional” in the CAR model is used because each element of the random process is specified conditionally on the values of the neighboring nodes. The CAR model is typically specified as

$$Z_i|\mathbf{z}_{-i} \sim \text{N}\left(\sum_{\forall c_{ij} \neq 0} c_{ij}z_j, m_{ii}\right), \quad \text{eqn 7}$$

where  $\mathbf{z}_{-i}$  is the vector of all  $Z_j$  where  $j \neq i$ ,  $\mathbf{C} = \rho\mathbf{W}$  is the spatial dependency matrix with  $c_{ij}$  as its  $i, j$ th element,  $c_{ii} = 0$ , and  $\mathbf{M}$  is zero except for diagonal elements  $m_{ii}$ . Note that  $m_{ii}$  may depend on the values in the  $i$ th row of  $\mathbf{C}$ . In this parameterization, the conditional mean of each

211  $Z_i$  is weighted by values at neighboring nodes. The variance component,  $m_{ii}$ , is also conditional on  
 212 the neighboring nodes and is thus nonstationary, varying with node  $i$ . In contrast to SAR models,  
 213 it is not obvious that (eqn 7) can lead to a full joint distribution for all random variables; however,  
 214 this was demonstrated by Besag (1974) using Brook's lemma (Brook, 1964) and the Hammersley-  
 215 Clifford theorem (Hammersley and Clifford, 1971; Clifford, 1990). For  $\mathbf{z}$  to have a proper statistical  
 216 distribution,  $(\mathbf{I} - \mathbf{C})^{-1}$  must exist and  $\mathbf{\Sigma} = \sigma_n^2(\mathbf{I} - \mathbf{C})^{-1}\mathbf{M}$  must be symmetric, which requires that

$$\frac{c_{ij}}{\tau_i^2} = \frac{c_{ji}}{\tau_j^2} \forall i, j. \quad \text{eqn 8}$$

217 For CAR models,  $\mathbf{W}$  and  $\rho$  are constrained in exactly the same way as for SAR models;  $\mathbf{W}$  must  
 218 be non-singular and  $1/\lambda_{[1]} < \rho < 1/\lambda_{[N]}$  for  $\lambda_{[1]}$  the smallest, and  $\lambda_{[N]}$  the largest eigenvalues of  
 219  $\mathbf{W}$ .

220 A special case of the CAR model, called the intrinsic autoregressive model (IAR) (Besag  
 221 and Kooperberg, 1995), occurs when the weights in (eqn 7) occur as,

$$Z_i \sim N \left( \sum_{j \in \mathcal{N}_i} z_j / |\mathcal{N}_i|, \tau^2 / |\mathcal{N}_i| \right), \quad \text{eqn 9}$$

222 where  $\mathcal{N}_i$  are all of the locations defined as neighbors of the  $i$ th location,  $|\mathcal{N}_i|$  is the number of  
 223 neighbors of the  $i$ th location, and  $\tau^2$  is a constant variance parameter. In (eqn 9), each random  
 224 variable is the average of its neighbors, and the variance is proportional to the inverse of the number  
 225 of neighbors. This idea, of creating weights based on averages of neighboring values, is discussed  
 226 next.

## 227 Row-standardization

228 Here, we begin a discussion of the weights matrix,  $\mathbf{W}$ , which applies to both SAR and CAR models.  
 229 Consider the simplest case, where a one in  $\mathbf{W}$  indicates a connection between sites  $i$  and  $j$  and a  
 230 zero indicates no such connection. For site  $i$ , let us suppose that there are  $|\mathcal{N}_i|$  neighbors, so there  
 231 are  $|\mathcal{N}_i|$  ones in the  $i$ th row of  $\mathbf{W}$ . Thinking in terms of constructing random variables, this means

232 that  $Z_i$  is the *sum* of its neighbors, and summing increases variance. Generally, if left uncorrected,  
 233 it will not be possible to obtain a covariance matrix in this case. As an analog, consider the first-  
 234 order autoregressive (AR1) model from time series, where  $Z_{i+1} = \phi Z_i + \nu_i$ , and  $\nu_i$  is an independent  
 235 random shock. It is well-known that  $\phi = 1$  is a random walk, and anything with  $|\phi| \geq 1$  will not  
 236 have a variance because the series “explodes” (e.g., Hamilton, 1994, pg. 53). There is a similar  
 237 phenomenon for SAR and CAR models. In our simple example, for the construction  $\rho \mathbf{W}$ , the value  
 238  $\rho |\mathcal{N}_i|$  effectively acts like  $\phi$ , and both should be less than 1 to yield a proper statistical model. For  
 239 example, consider the case where all locations are on an evenly-spaced rectangular grid of infinite  
 240 size where each node is connected to 4 neighbors, called a rook’s neighborhood; one each up, down,  
 241 left, and right. It is well-known that spatial autoregressive models for this example must have  
 242  $|\rho| < 1/4$  (Haining, 1990, pg. 82). More generally,  $|\rho| < 1/n$  if all sites have exactly  $n$  neighbors,  
 243  $|\mathcal{N}_i| = n \forall i$ , to keep variance under control. This leads to the idea of row-standardization.

244 If we divide each row in  $\mathbf{W}$  by  $w_{i,+} \equiv \sum_j w_{ij}$ , then, again thinking in terms of constructing  
 245 random variables, each  $Z_i$  is the *average* of its neighbors, which decreases variance. In general then,  
 246 regardless of the number of neighbors, when using row standardization it is sufficient for  $|\rho| < 1$ ,  
 247 which is very convenient. Row standardization simplifies the bounds of  $\rho$  and makes optimization  
 248 easier to implement. Moreover, consider again the case of an evenly-spaced rectangular grid of  
 249 points, but this time of finite size, again using a rook’s neighborhood. Using row standardization,  
 250 points in the interior of the rectangle are averaged over 4 neighbors, and they will have smaller  
 251 variance than those at the edges, averaged over 3 neighbors, and the highest variance will be  
 252 locations in the corners, averaged over 2 neighbors. Hence, in general, variance increases toward  
 253 the *edges*. Without row standardization, even when  $\rho$  controls overall variance, locations in the  
 254 *middle*, summed over more neighbors, have higher variance than those at the edges. For an error  
 255 process in (eqn 1), higher variance near the edges makes more sense, and, with a more natural and  
 256 consistent range of values for  $\rho$ , we highly recommend row-standardization. For the CAR models,  
 257 if  $\mathbf{W}_+$  is an asymmetric matrix with each row in  $\mathbf{W}$  divided by  $w_{i,+}$ , then  $m_{ii} = \tau^2/w_{i,+}$  (the  $i$ th  
 258 diagonal element of  $\mathbf{M}$ ) satisfies (eqn 8), and note that  $\tau^2$  will not be identifiable from  $\sigma_Z^2$  in (eqn

3), so the row-standardized CAR model can be written equivalently as,

$$\mathbf{\Sigma} = \sigma_Z^2(\mathbf{I} - \rho\mathbf{W}_+)^{-1}\mathbf{M}_+ = \sigma_Z^2(\text{diag}(\mathbf{W}\mathbf{1}) - \rho\mathbf{W})^{-1}. \quad \text{eqn 10}$$

Using row-standardization, and setting  $\rho = 1$  in (eqn 7) leads to (eqn 9). In our AR1 analogy, this is equivalent to  $\phi = 1$ . In this case,  $\mathbf{\Sigma}^{-1}$  is singular (i.e., does not have an inverse), and  $\mathbf{\Sigma}$  does not exist. While this may seem undesirable, random walks and Brownian motion are stochastic processes without covariance matrices. Considering how they are constructed, it helps to think of the variances and covariances being defined on the increments; the differences between adjacent variables. For these increments, the variances and covariances are well-defined. The IAR distribution is improper, however it is similarly well-defined on spatial increments or contrasts. To make the IAR proper, an additional constraint can be included,  $\sum_i Z_i = 0$ . In essence, this constraint allows all of the random effects to vary except one, which is subsequently used to ensure that the values sum to zero as a whole. Geometrically, the sum-to-zero constraint can be thought of as anchoring the process near zero for the purposes of random errors in a model. With such a constraint, the IAR model is appealing as an error process (eqn 1) that is a flexible surface and there is no autocorrelation parameter to estimate.

### More Weighting – Separating Functional from Structural Connectivity

So far, we have reviewed standard spatial autoregressive models. Now, we want to consider their more general formulation as graphical, or network models. In general (other scientific and statistical literature), the autoregressive component is an “error” process, and not really of intrinsic interest (compared to prediction or estimating fixed effects parameters,  $\beta$ ). However, for ecological networks, there is a great deal of interest in studying spatial connectivity, or equivalently spatial autocorrelation. Here, we discuss other weighting schemes for autoregressive models that have been very rarely, or never, used, but would provide valid autocorrelation models for studying connectivity in ecology. In particular, although the decomposition is not unique, we introduce weighting schemes for the  $\mathbf{W}$  matrix that can separate and clarify structural and functional components in

network connectivity. By structural, we mean correlation that is determined by neighborhoods, distance, etc., and by functional, we mean correlation that is affected by measured covariates of interest, which we illustrate next.

Consider a spatial network of nodes and edges, with the response variable measured at nodes, putting us in the setting of SAR and CAR models. Let  $\mathbf{e}_{ij}$  be a characteristic of an edge. The structural idea can be contained in the neighborhood structure – the binary representation of connectivity contains the idea of neighborhood structure. Then edge weights,  $w_{ij}$ , between the  $i$ th and  $j$ th nodes could combine functional and structural connectivity if they are modeled as,

$$w_{ij} = \begin{cases} f(\mathbf{e}_{ij}, \boldsymbol{\theta}), & j \in \mathcal{N}_i \\ 0, & j \notin \mathcal{N}_i. \end{cases} \quad \text{eqn 11}$$

where  $\boldsymbol{\theta}$  is a  $p$ -vector of parameters. To clarify, consider the case where  $\mathbf{x}_i$  is a vector of  $p$  habitat characteristics of the  $i$ th node,  $\mathbf{e}_{i,j} = (\mathbf{x}_i + \mathbf{x}_j)/2$ , and  $f(\mathbf{e}_{ij}, \boldsymbol{\theta}) = \exp(\mathbf{e}_{ij}'\boldsymbol{\theta})$  (Hanks and Hooten, 2013). This allows a model of the effect that habitat characteristics at the nodes has on connectivity. If  $\theta_h < 0$ , then an increase in the  $h$ th habitat characteristic results in a smaller edge weight and greater resistance to network connectivity. However, if  $\theta_h > 0$ , then an increase in the  $h$ th habitat characteristic results in a larger edge weight and less resistance to network connectivity. In this example, the mean of the habitat characteristics found at the two nodes,  $(\mathbf{x}_i + \mathbf{x}_j)/2$ , was used, but any other function of the two values could also be used (e.g., difference) if it makes ecological sense. Alternatively,  $f(\mathbf{e}_{ij}, \boldsymbol{\theta})$  could be something that is directly measured on edges, such as a sum of pixel weights in a shortest path between two nodes from a habitat map.

For a matrix representation of (eqn 11), let  $\mathbf{F}(\boldsymbol{\theta})$  be a matrix of functional relationships for all edges, let  $\mathbf{B}$  be a binary matrix indicating neighborhood structure, and  $\mathbf{W} = \mathbf{F}(\boldsymbol{\theta}) \odot \mathbf{B}$ , where  $\odot$  is the Hadmard (direct, or element by element) product. Then  $\mathbf{F}(\boldsymbol{\theta}) \odot \mathbf{B}$  allows a decomposition for exploring structural and functional changes in connectivity by manipulating each separately. Of course, this must respect the restrictions described above for SAR and CAR models, and the parameters need to be estimated, which we discuss in the section on inference.

## Comparison of CAR to SAR and Practical Guidelines

With a better understanding of SAR and CAR models, we now compare them more closely and make practical recommendations for their use; see also Wall (2004). First, we do not recommend versions of the SAR model given by (eqn 5) and (eqn 6). It is difficult to understand how smoothing/lagging covariates and extra random effects contributes to model performance, nor to our understanding, and these models performed poorly in ecological tests (Dormann et al., 2007; Kissling and Carl, 2008). Henceforth, we only discuss the error model defined by (eqn 4).

It is well-known that any SAR model can be written as a CAR model, and Cressie (1993, pg. 408) demonstrates how a SAR model with 4 neighbors (rook’s neighbor) results in a CAR model that involves all eight neighbors (queen’s neighbor) plus rook’s move to the second neighbors. Although it does not appear to be as simple to go from a CAR model to a SAR, contrary to published accounts (Cressie, 1993, pg. 408) and (Banerjee et al., 2004, pg. 86)), it is possible (but not uniquely, without further conditions, which we demonstrate in Appendix B). In fact, it is evident from (eqn 2) that specifying first-order neighbors in  $\mathbf{B}$  will result in non-zero partial correlations between second-order neighbors because of the product  $(\mathbf{I} - \mathbf{B})(\mathbf{I} - \mathbf{B})$ . Hence, SAR models have a reputation as being less “local” than the CAR models. In fact, using the same construction  $\rho\mathbf{W}$  for both SAR and CAR models, Wall (2004) shows that correlation (in  $\Sigma$ , not partial correlation) increases more rapidly with  $\rho$  in SAR models than CAR models.

Regarding restrictions on  $\rho$ , Wall (2004) also shows there is very strange behavior for negative values of  $\rho$ . In geostatistics, there are very few models that allow negative spatial autocorrelation, and, when they do, it cannot be strong. The fact that  $\mathbf{W}$  in SAR models is not required to be symmetric may seem to be an advantage over CAR models. However, we point out that this is illusory from a modeling standpoint, although it may help conceptually in formulating the models. For an analogy, again consider the AR1 model from time series. The model is specified as  $Z_{i+1} = \phi Z_i + \nu_i$ , so it seems like there is dependence only on previous times. However, the correlation matrix is symmetric, and  $\text{corr}(Z_i, Z_{i+t}) = \text{corr}(Z_i, Z_{i-t}) = \phi^t$ . Note also that this shows that specifying partial correlations as zero (or conditional independence), does not mean that marginal correlation is zero (i.e.,  $\text{corr}(Z_i, Z_{i+t}) \neq 0$  for all  $t$  lags. The same is true for CAR and SAR models.

335 In fact, the situation is less clear than for the AR1 models, where  $\text{corr}(Z_i, Z_{i+t}) = \phi^t$  regardless  
 336 of  $i$ . For CAR and SAR models, two sites that have the same “distance” from each other will  
 337 have different correlation, depending on whether they are near the center of the spatial network,  
 338 or near the edge; that is, correlation is nonstationary, just like the variance when we described  
 339 row-standardization.

## 340 CAR and SAR in Hierarchical Models

341 We now turn our focus to the use of CAR and SAR spatial models within a hierarchical model.  
 342 To discuss these models more specifically and concretely, in the example and following discussion,  
 343 consider the following hierarchical structure that forms a general framework for all that follows,

$$\begin{aligned}
 \mathbf{y} &\sim [\mathbf{y}|g(\boldsymbol{\mu}), \boldsymbol{\nu}], \\
 \boldsymbol{\mu} &\equiv \mathbf{X}\boldsymbol{\beta} + \mathbf{z} + \boldsymbol{\varepsilon}, \\
 \mathbf{z} &\sim [\mathbf{z}|\boldsymbol{\Sigma}] \equiv \text{N}(\mathbf{0}, \boldsymbol{\Sigma}), \\
 \boldsymbol{\Sigma}^{-1} &\equiv \mathbf{F}(\mathbf{N}, \mathbf{D}, \rho, \boldsymbol{\theta}, \dots), \\
 \boldsymbol{\varepsilon} &\sim [\boldsymbol{\varepsilon}|\sigma^2] \equiv \text{N}(\mathbf{0}, \sigma^2\mathbf{I}),
 \end{aligned}
 \tag{eqn 12}$$

344 where  $[\cdot]$  denotes a statistical distribution. Here, let  $\mathbf{y}$  contain random variables for the potentially  
 345 observable data, which could be further partitioned into  $\mathbf{y} = (\mathbf{y}'_o, \mathbf{y}'_u)'$ , where  $\mathbf{y}_o$  are observed  
 346 and  $\mathbf{y}_u$  are unobserved. Then  $[\mathbf{y}|g(\boldsymbol{\mu}), \boldsymbol{\nu}]$  is typically the data model, with a distribution such as  
 347 Normal (continuous ecological data, such as plant biomass), Poisson (ecological count data, such  
 348 as animal abundance), or Bernoulli (ecological binary data, such as occupancy), which depends  
 349 on a mean  $\boldsymbol{\mu}$  with link function  $g$ , and other parameters  $\boldsymbol{\nu}$ . The mean  $\boldsymbol{\mu}$  has the typical spatial  
 350 linear mixed model form, with design matrix  $\mathbf{X}$  (containing covariates, or explanatory variables),  
 351 regression parameters  $\boldsymbol{\beta}$ , spatially autocorrelated errors  $\mathbf{z}$ , and independent errors  $\boldsymbol{\varepsilon}$ . We let the  
 352 random effects,  $\mathbf{z}$ , be a zero mean multivariate normal distribution with covariance matrix  $\boldsymbol{\Sigma}$ . In a  
 353 geostatistical spatial-linear model, we would model  $\boldsymbol{\Sigma}$  directly with covariance functions based on  
 354 distance like the exponential, spherical and Matern (Chiles and Delfiner, 1999). The variance  $\sigma^2$ ,  
 355 of the independent component  $\text{var}(\boldsymbol{\varepsilon}) = \sigma^2\mathbf{I}$ , is called the nugget effect. However, in CAR and SAR



models, and as described above, we model the inverse of the covariance matrix,  $\Sigma^{-1}$ , also called the precision matrix. We denote this as a matrix function,  $\mathbf{F}$ , that depends on other information (e.g., a neighborhood matrix  $\mathbf{N} = \mathbf{B}$  or  $\mathbf{C}$ , a distance matrix  $\mathbf{D}$ , and perhaps others). We isolate the parameter  $\rho$  that controls the strength of autocorrelation, and there could be other parameters contained in  $\boldsymbol{\theta}$ , that form the functional relationships among  $\mathbf{N}, \mathbf{D}, \dots$ , and  $\Sigma^{-1}$ . In a Bayesian analysis, we could add further priors, but here we provide just the essential model components that provide most inferences for ecological data. The model component to be estimated or predicted from (eqn 12) is identified in Table 1. Note that a full joint distribution for all random quantities can be written as  $[\mathbf{y}|g(\boldsymbol{\mu}), \boldsymbol{\nu}][\mathbf{z}|\boldsymbol{\Sigma}][\boldsymbol{\varepsilon}|\sigma^2]$ , but the only observable data are  $\mathbf{y}$ . The term likelihood is used when the joint distribution is considered a function of all unknowns, given the observed data, which we denote  $L(\mathbf{y}|\cdot)$ .

## Fitting Methods for Autoregressive Models

Maximum likelihood estimation is one of the most popular estimation methods (Cressie, 1993). Earlier, when computers were less powerful, methods were devised to trade efficiency for speed, such as pseudolikelihood (Besag, 1975) and coding (Besag, 1974) for CAR models, among others (Cressie, 1993). Both CAR and SAR models are well-suited for maximum likelihood estimation (Banerjee et al., 2004). For spatial models, the main computational burden in geostatistical models is inversion of the covariance matrix; for CAR and SAR models, the inverse is what we actually model. Thus, only the determinant of the covariance matrix needs computing, and fast sparse matrix methods can be used (Pace and Barry, 1997a,b). If matrices need inverting, sparse matrix methods can be used (Rue and Held, 2005). In addition, for Bayesian Markov chain Monte Carlo methods (MCMC, Gelfand and Smith, 1990), CAR models are ready-made for conditional sampling because of their conditional specification.

The spatial autoregressive models are often used in generalized linear models, which can be viewed as hierarchical models, where the spatial CAR model is generally latent in the mean function in a hierarchical modeling framework. Indeed, one of their most popular uses is for “disease-mapping,” whose name goes back to Clayton and Kaldor (1987); see Lawson (2013) for

book-length treatment. These models can be treated as hierarchical models (Cressie et al., 2009), where the data are assumed to be a count model, such as Poisson, but then the log of the mean parameter has a CAR/SAR model to allow for extra-Poisson variation that is spatially patterned (e.g., Ver Hoef and Jansen, 2007). A similar hierarchical framework has been developed as a generalized linear model for occupancy, which is a binary model, but then the logit of the mean parameter has a CAR/SAR model to allow for extra-binomial variation that is spatially patterned (Magoun et al., 2007; Gardner et al., 2010; Johnson et al., 2013; Broms et al., 2014; Poley et al., 2014). CAR and SAR models can be embedded in more complicated hierarchical models as well (e.g., Ver Hoef et al., 2014). Sometimes that may be too slow, and a fast general-purpose approach to fitting these types of hierarchical models, which depend in part on the sparsity of the CAR covariance matrix, is integrated nested Laplace approximation (INLA, Rue et al., 2009), which has been used in generalized linear models for ecological data (e.g., Haas et al., 2011; Aarts et al., 2013) and spatial point patterns (Illian et al., 2013), among others. INLA provides fast computing for approximate Bayesian inference on the marginal distributions of latent variables.

## EXAMPLE

We used trends in harbor seals (*Phoca vitulina*) for an example to illustrate the models and approaches for inference described earlier. The study area is shown in Fig. 1 and contains 463 polygons along the mainland, and around islands, in Southeast Alaska. Based on genetic sampling, this area has been divided into 5 different “stocks” (or genetic populations). Over a 14 year period, at various intervals per polygon, seals were counted from aircraft. Using those counts, a trend for each polygon was estimated using Poisson regression. Any polygons with less than two surveys were eliminated, along with trends (linear on the log scale) that had estimated variances greater than 0.1. This eliminated sites with small sample sizes. Going forward, we will treat the estimated trends, on the log scale, as raw data, and ignore the estimated variances. These data were chosen to be illustrative because we expect the trends to show geographic patterns (more so than abundance which varied widely in polygons), and perhaps differences in mean rates and connectivity

409 due to stock structure. The data are also continuous in value, so we model the trends with normal  
410 distributions to keep the modeling simpler and the results more evident. A map of the raw trend  
411 values is given in Fig. 2, showing 463 polygons, of which 306 had observed values and 157 were  
412 missing.

413 For neighborhood structures, we considered three levels of neighbors. The first-order neigh-  
414 bors were based on any two polygons sharing one or more boundary point, and were computed  
415 using the *poly2nb* function in the *spdep* package (Bivand and Piras, 2015) in R (R Core Team,  
416 2014). Some polygons were isolated, so they were manually connected to the nearest polygon in  
417 space using straight-line (Euclidean) distance between polygon centroids. The first-order neighbors  
418 are shown graphically in Fig. 3a with a close-up of part of the study area given in Fig. 3b. If  $\mathbf{N}_1$  is  
419 a matrix of binary values, where a 1 indicates two sites are first-order neighbors, and a 0 otherwise,  
420 then second-order neighbors, to include neighbors of first-order neighbors, were easily obtained in  
421 the matrix  $\mathbf{N}_2 = \mathcal{I}(\mathbf{N}_1^2)$ , where  $\mathcal{I}(\cdot)$  is an indicator function on each element of the matrix, being 0  
422 only when that element is 0, and 1 otherwise. A close-up of some of the second-order neighbors is  
423 shown in Fig. 3c. The fourth-order neighbor matrix was obtained as  $\mathbf{N}_4 = \mathcal{I}(\mathbf{N}_2^2)$ , and a close-up  
424 is shown in Fig. 3d.

425 We considered covariance constructions that elaborated the three different neighborhood  
426 definitions. Let  $\mathbf{N}_i; i = 1, 2, 4$  be a neighborhood matrix as described in the previous paragraph.  
427 Let  $\mathbf{S}$  be a matrix of binary values that indicate whether two sites are in different stocks; that is,  
428 if site  $i$  and  $j$  are in the same stock, then  $\mathbf{S}[i, j] = 0$ , otherwise  $\mathbf{S}[i, j] = 1$ . Finally, let the  $i, j$ th  
429 entries in  $\mathbf{D}$  be the Euclidean distance between the centroids of the  $i$ th and  $j$ th polygons. Then  
430 the most elaborate CAR/SAR model we considered was

$$\mathbf{W} = \mathbf{N}_i \odot \mathbf{F}(\boldsymbol{\theta}) = \mathbf{N}_i \odot \exp(-\mathbf{S}/\theta_1) \odot \exp(-\mathbf{D}/\theta_2). \quad \text{eqn 13}$$

431 We use (eqn 13) in (eqn 2) and (eqn 3), where for SAR models  $\mathbf{B} = \rho\mathbf{W}$  or  $\mathbf{B} = \rho\mathbf{W}_+$ , and for  
432 CAR models  $\mathbf{C} = \rho\mathbf{W}; \mathbf{M} = \mathbf{I}$  or  $\mathbf{C} = \rho\mathbf{W}_+; \mathbf{M} = \mathbf{M}_+$ . Note that when considering the spatial  
433 regression model in (eqn 1),  $\text{var}(\mathbf{y}) = \boldsymbol{\Sigma} + \sigma_\varepsilon^2\mathbf{I}$  would also be possible; for example, for a first-

order CAR model,  $\text{var}(\mathbf{y}) = \sigma_Z^2(\mathbf{I} - \rho\mathbf{W})^{-1} + \sigma_\varepsilon^2\mathbf{I}$ . However, when  $\rho = 0$ , then  $\sigma_Z^2$  and  $\sigma_\varepsilon^2$  are not identifiable. In fact as  $\rho$  goes from 1 to 0 it allows for diagonal elements to dominate in  $(\mathbf{I} - \rho\mathbf{W})^{-1}$ , and there seems little reason to add  $\sigma_\varepsilon^2\mathbf{I}$ . We tried some models with the additional component  $\sigma_\varepsilon^2\mathbf{I}$ , but  $\sigma_\varepsilon^2$  was always estimated to be near 0, so few of those models are presented. The exception is the IAR model, where conceptually  $\rho$  is fixed at one.

Our construction is unusual due to the  $\exp(-\mathbf{S}/\theta_1)$  component. We interpret  $\theta_1$  as an among-stock connectivity parameter. Connectivity is of great interests to ecologists, and by its very definition it is about relationships *between* two items. Therefore, it is naturally modeled through the covariance matrix, which is also concerned with this *second-order* model property. Recall that, within stock, all entries in  $\mathbf{S}$  will be zero, and hence those same entries in  $\exp(-\mathbf{S}/\theta_1)$  will be one. Now, if *among* stocks there is little correlation, then  $\theta_1$  should be very small, causing those entries in  $\exp(-\mathbf{S}/\theta_1)$  to be near zero. On the other hand, if  $\theta_1$  is very large, then there will be high correlation among stocks, and so the stocks are highly connected with respect to the behavior of the response variable, justifying our interpretation of the parameter. When used in conjunction with the neighborhood matrix, the  $\exp(-\mathbf{S}/\theta_1)$  component helps determine if there is additional correlation due to stock structure (low values of  $\theta_1$ ) or whether the neighborhood definitions are enough ( $\theta_1$  very large).

We fit model (eqn 1) with a variety of fixed effects and covariance structures, and a list of those models is given in Table 2. We fit models using maximum likelihood, and details are given in Appendix C. The resulting maximized value of  $2*\log\text{-likelihood}$  is given in Fig. 4. Of course, some models are generalizations of other models, with more parameters, and will necessarily have a better fit. Methods such as Akaike Information Criteria (AIC, Akaike, 1973), Bayesian Information Criteria (BIC, Schwarz, 1978), or others (see, e.g., Burnham and Anderson, 2002; Hooten and Hobbs, 2015), can be used to select among these models. This is an example of objective 1 listed in Table 1. For AIC, each additional parameter adds a “penalty” of 2 for  $2*\log\text{-likelihood}$ , so number of model parameters are shown along the x-axis, and dashed lines at increments of two help evaluate models in Fig. 4. If one prefers a likelihood-ratio approach, then a model with one more parameter should be better by a  $\chi$ -squared value on 1 degree of freedom, or 3.841. We note that there appears

to be high variability among model fits, depending on the neighborhood structure (Fig. 4). Several authors have decried the general lack of exploration of the effects of neighborhood definition and choice in weights (Best et al., 2001; Earnest et al., 2007), and our results support their contention that this deserves more attention. In particular, it is interesting that row-standardized CAR models give substantially better fits than unstandardized, and CAR is much better than SAR. Also, for row-standardized CAR models, fit worsens going from first-order to second-order neighborhoods, but then gets better when going to fourth-order. Also, perhaps not surprising, using distance between centroids had little effect until fourth-order neighborhoods were used. By an AIC criteria, model XC4RD would be the best model. For model XC4RDS, the parameter  $\theta_1$  was very large, making  $\exp(-\mathbf{S}/\theta_1)$  constant at 1, so this model component could be dropped without changing the likelihood. Also, the addition of the uncorrelated random errors (model XC4RDU) had an estimated variance  $\varepsilon^2$  near zero, and left the likelihood essentially unchanged.

As an example of objective 2 from Table 1, the estimation of fixed effects parameters, for 3 different models, are given in Table 3. The model is overparameterized, so the parameter  $\mu$  is essentially the estimate for stock 1. For example, for the XU model,  $\exp(-0.079) = 0.92$ , giving an estimated trend of about 8% average decrease per year for sites from stock 1. It is significantly different from 0, which is equivalent to no trend, at  $\alpha = 0.05$ . This inference is obtained by taking the estimate and dividing by the standard error, and then assuming that is a standard normal distribution under the null hypothesis that  $\mu = 0$ . The other estimates are *deviations* from  $\mu$ , so stock 2 is estimated to have  $\exp(-0.079 + 0.048) = 0.97$ , or a decrease of about 3% per year. A  $P$ -value for stock 2 is obtained by assuming that the estimate divided by the standard error has a standard normal distribution under the model of no difference in means, which is 0.111, and is interpreted as the probability of obtaining the stock 2 value, or larger, if it had the same mean as stock 1. It appears that stocks 3–5 have increasing trends, and that they are significantly different from stock 1 at  $\alpha = 0.05$ . In comparison, model XC4R, using maximum likelihood estimates (mle), and Bayesian estimates (mcmc), are given in the middle two sets of columns of Table 3. Notice that for both, the standard errors are larger than for the independence model XU, leading to greater uncertainty about the fixed effects estimates. Also, the Bayesian standard errors are somewhat

larger than those of maximum likelihood. This is often observed in spatial models when using Bayesian methods, where the uncertainty in estimating the covariance parameters is expressed in the standard errors of the fixed effects, whereas for MLE the covariance parameters are fixed at their most likely values. The MLE estimates and standard errors for the best-fitting model, according to AIC (model XC4RD), are shown in the last set of columns in Table 3, which are very similar to the XC4R model. Further contrasts between trends in stocks are possible by using the variance-covariance matrix for the estimated fixed effects for MLE estimates, or finding the posterior distribution of the contrasts using MCMC sampling in a Bayesian approach.

For objective 3 from Table 1, consider the curves in Fig. 5. We tried all combinations of CAR and SAR models, with and without row-standardization, for the first-, second-, and fourth-order neighbors (12 possible models). All such models had 7 parameters, and a few of the models are listed in Table 2. The likelihood profiles for  $\rho$  of the three best-fitting models are shown in Fig. 5. The peak value for XC4R shows that this is the best model, and the MLE for  $\rho$  for this model is 0.604. This curve also provides a likelihood-based confidence interval, known as a profile likelihood confidence interval (Box and Cox, 1964), which essentially inverts a likelihood-ratio test. A  $100(1 - \alpha)\%$  confidence interval for a given parameter is the set of all values such that a two-sided test of the null hypothesis that the parameter is the maximum likelihood value would not be rejected at the  $\alpha$  level of significance; i.e., the MLE value minus a chi-squared value with one degree of freedom, which is 3.841 if  $\alpha = 0.05$ . These are all values above the dashed line in Fig. 5 for model XC4R, or, in other words, the endpoints of the confidence interval are provided by the intersection of the dashed line with the curve, which has a lower bound of 0.113 and an upper bound of 0.868. We also show the posterior distribution of  $\rho$  for the same model, XC4R, using a Bayesian analysis. The posterior mean was 0.687, with a 95% credibility interval ranging from 0.315 to 0.933. The Bayesian estimate used noninformative priors, so the joint posterior distribution of all parameters will be proportional to the likelihood. The difference between the MLE and the Bayesian estimates for the XC4R model is due to the fact that the MLE is the peak of the likelihood jointly (with all other parameters at their peak), whereas the Bayesian posterior is a marginal distribution (all other parameters have essentially been integrated over by the MCMC algorithm). Nonetheless, the

MLE and Bayesian inferences are quite similar.

Fig. 6 shows likelihood profiles for the other parameters in the covariance matrix. For the best model, XC4RD, the solid line in Fig. 6a shows a peak for  $\log(\theta_2)$  at 3.717, forming the maximum likelihood estimate and relating to objective 4 from Table 1. Once again, we show a dashed line at the maximized  $2\log$ -likelihood (413.447) minus a chi-squared value at  $\alpha = 0.05$  on one degree of freedom (3.841) to help visualize a confidence interval for  $\theta_2$ ; i.e., the profile likelihood confidence interval given by all values of the solid line that are above the dashed line. The loglikelihood drops rapidly from the MLE  $\hat{\theta}_2 = 3.717$  on the left, intersecting the dashed line and forming a lower bound at 2.894, whereas the upper limit is unbounded. We return to the notion of stock connectivity in Fig. 6b. The profile likelihood for  $\theta_1$  for Model XC4RDS is given by the solid line. The likelihood is very flat for larger values of  $\theta_1$ , and in fact it is continuously increasing at an imperceptible rate. Thus, the MLE is the largest value in the parameter range, which we clipped at  $\log(\theta_1) = 10$ . A lower bound is at  $\log(\theta_1) = 0.525$ , whereas the upper limit is unbounded again.

Continuing with further inferences from the model, we consider prediction (objective 5) from Table 1. Algorithms for both prediction and smoothing are given in Appendix D. Kriging is a spatial prediction method associated with geostatistics (Cressie, 1990). However, for any covariance matrix, the prediction equations can be applied regardless of how that covariance matrix was developed. We used universal kriging, that is, we included stock effects as covariates, (Huijbregts and Matheron, 1971; Cressie, 1993, pg. 151) to predict all unsampled polygons (black polygons in Fig. 2) using the XC4RD model. Note that kriging, as originally formulated, is an exact interpolator (Cressie, 1993, pg. 129) that “honors the data” (Schabenberger and Gotway, 2005, p. 252) by having predictions take on observed values at observed sites. In Fig. 7a we show the raw observations along with the predictions, making a complete map for all sites. Of course, what distinguishes predictions using statistical models, as opposed to deterministic algorithms (e.g., inverse distance weighted, Shepard, 1968) is that statistical predictions provide standard errors for each prediction (Fig. 7B). When kriging is used as an exact interpolator, the values are known at observed sites, so the prediction variances are zero at observed sites. Hence, we only show the prediction standard errors for polygons with missing data.

We also use the more traditional smoother for CAR and SAR models, such as those used in (Clayton and Kaldor, 1987), forming objective 6 from Table 1. For model XC4RD, without any independent component, this is essentially equivalent to leave-one-out-cross-validation. That is, the conditional expectation, which is obtained directly from (eqn 7) (after adjusting for estimated covariate effects) is used rather than the observed value at each location. Once the covariance matrix is known, for normally distributed data, ordinary kriging is also the conditional expectation (Cressie, 1993, p. 108, 174). Hence, the predicted and smoothed values, using the conditional expectation, are given in Fig. 7c; note then that the predictions are equivalent to Fig. 7a at the unsampled locations. Two extremes in smoothing approaches are 1) kriging as an exact predictor, that is, it leaves the data unchanged (Figs. 7a), and 2) removing observed data to replace them with conditional expectations based on neighbors (Fig. 7c). In fact, both are quite unusual for a smoothing objective. Generally, a model is adopted with a spatial component, and a noisy measurement error or independent component. Smoothing then involves finding a compromise between the spatial component and the raw, observed data. As an example for these data, consider the XI4RU model, which has an IAR component plus an uncorrelated error component. The IAR model has very high autocorrelation ( $\rho = 1$ ), but here we allowed it to be a mixture with uncorrelated error, and the relative values of  $\sigma_Z^2$  and  $\sigma_\varepsilon^2$  will determine how much autocorrelation is estimated for the data. Under this model, predictions for observed data can fall between the very smooth IAR predictions and the very rough observed data. When such a model is formulated as a hierarchical model (eqn 12), often in a Bayesian context, predictions will exhibit a property called shrinkage (Fay and Herriot, 1979), where predictions of observed values are some compromise between an ultra-smooth fit from a pure IAR model, and the roughness of the raw data (Fig. 7d). The amount of shrinkage depends on the relative values of  $\sigma_Z^2$  and  $\sigma_\varepsilon^2$ . In fact, this is usually the case when CAR and SAR models are used in a generalized linear model setting because the conditional independence assumption (e.g., of a Poisson distribution) is analogous to the  $\sigma_\varepsilon^2 \mathbf{I}$  component. Note that a Bayesian perspective is not a requirement, a similar objective is obtained using filtered kriging (Waller and Gotway, 2004, pg. 306) when there are both spatial and uncorrelated variance components.



Finally, to complete the example, we return to the idea of nonstationarity in variances and covariances. Notice that, as claimed earlier, row-standardization causes variance to decrease with the numbers of neighbors (which are generally greater in the interior of a study area in contrast to the edges) for model XC4R (Fig. 8a), but it is not a simple function of neighbors alone, as it depends in complicated ways on the whole graphical (or network) structure. In contrast, variance generally increases with the number of neighbors without row-standardization (model XC4) of the neighborhood matrix (Fig. 8a). Correlation also decreases with neighbor order, although not as dramatically as one might expect (Fig. 8b), and not at all (on average) between first-order to second-order when the neighborhood matrix is not row-standardized. Box plots summarize all possible correlations as a function of distance between centroids (binned into classes, Fig 8c,d), which show that while correlation generally decreases with distance between centroids, there is a great deal of variation. Also recall that the MLE for  $\rho$  for model XC4R was 0.604 (Fig. 5) for the inverse covariance matrix, but for the covariance matrix, correlations are much lower (Fig. 8b-d). Because weights are developed for partial correlations, or for the inverse of the covariance matrix, when we examine the covariance matrix itself, the diagonal elements are non-constant, in contrast to typical geostatistical models. It is important to realize that there is no direct calculation between the estimated  $\rho$  value in the CAR or SAR model and the correlations in the covariance matrix; only that higher  $\rho$  generally means higher correlations throughout the covariance matrix. One can always invert the fitted CAR or SAR model to obtain the full covariance matrix, and this can then be inspected and summarized if needed (e.g. Fig. 8), and we highly recommend it for model diagnostics and a better understanding of the fitted model.

## DISCUSSION AND CONCLUSIONS

We have given six objectives used for spatial autoregressive models, some of which are common, and others less so. We argued that the development of the weights in modeling the covariance matrix for CAR and SAR models is less intuitive than choosing a covariance model in geostatistics, but some intuition can be gained by considering the relationship to partial correlations. We also

argued that row standardization is generally a good idea after choosing initial neighborhoods and weights. CAR models will generally be more “local” for a given set of neighbors because, for that same set of neighbors, the SAR model squares the weights matrix, creating neighbors of neighbors in the inverse covariance matrix. The IAR model is a special case of the CAR model that uses row standardization and where the autocorrelation parameter is fixed at one, which leads to an improper covariance matrix; however, much like a similar AR1 model, or Brownian motion, these are still useful models. We used an example data set by fitting a variety of CAR/SAR models using MLE and MCMC methods to illustrate all six objectives outlined in the Introduction. Here, we give further discussion on 5 additional take-home messages: 1) thoughts on choosing between CAR and IAR models, 2) modeling ecological effects in the covariance matrix, 3) the appeal of spatial smoothing, 4) how to handle isolated neighbors, and 5) software considerations.

The choice of IAR versus CAR is confusing, and while both are often described in the literature together, there is little guidance on choosing between them. The IAR has one less parameter to estimate. It was proposed by Besag and Kooperberg (1995) in part based on the following: they noticed that for a certain CAR model,  $\rho$  in (eqn 3) needed to be 0.999972 in order to have a marginal correlation of near 0.75 (indeed, compare the estimate of  $\hat{\rho} = 0.604$  in our example yielding the correlations seen in Fig. 8). In many practical applications,  $\rho$  was often estimated to be very near 1, so Besag and Kooperberg (1995) suggested the IAR model as a flexible spatial surface that has one less parameter to estimate. On the other hand, critics complained that it may force spatial smoothness where none exists (e.g., Leroux et al., 2000). Our point of view is best explored through the hierarchical model (eqn 12). Consider an example of count data, where the data model,  $\mathbf{y} \sim [\mathbf{y}|g(\boldsymbol{\mu})]$ , conditional on the mean  $g(\boldsymbol{\mu})$ , is composed of independent Poisson distributions. Hence, there is no extra variance parameter  $\boldsymbol{\nu}$ , but rather the independent, nonstationary variance component is already determined because it is equal to the mean. In this case, we recommend the CAR model to allow flexibility in modeling the diagonal of the covariance matrix (the CAR model can allow for smaller  $\rho$  values, which essentially allows for further uncorrelated error). On the other hand, if  $[\mathbf{y}|g(\boldsymbol{\mu}), \boldsymbol{\nu}]$  has a free variance parameter in  $\boldsymbol{\nu}$  (e.g., the product of independent normal or negative binomial distributions), then we recommend

the IAR model to decrease confounding between the diagonal of  $\Sigma$ , essentially controlled by  $\rho$ , and the free variance parameter in  $\nu$ .

The results for Figs. 5 and 6 have confidence intervals that are quite wide. We believe that, in general, uncertainty is much higher when trying to estimate covariance parameters than regression (fixed effect) parameters. Nevertheless, the covariance models that we constructed demonstrate that it is possible to examine the effect of covariates in the covariance structure. In other words, it is possible to make inference on connectivity types of parameters in the covariance matrix, but, secondly, they may be difficult to estimate with much precision if the data are measured only on the nodes. In our example, when stock effects were put into the mean structure, there was abundant evidence of different effects, but when that effect was put into the covariance matrix, the precision was quite low. It is important to put connectivity effects into the covariance matrix (in many cases, that will be the only place that makes sense), but realize that they may be hard to estimate well without a lot of data.

From an ecological viewpoint, why do spatial smoothing? In geology, and mining in particular, modelers were often adamant that no smoothing occur (honoring the data). Notice from Fig. 2 that the largest value is 0.835 from the legend on the right. Recalling that these are trends, on the log scale, that means that the observed value from the data was  $\exp(0.835) = 2.3$ , or more than doubling each year. That is clearly not a sustainable growth rate and is likely due to small sample sizes and random variation. That same value from Fig. 7c is  $\exp(0.039) = 1.04$ , or about 4% growth per year, which is a much more reasonable estimate of growth. The largest smoothed value in Fig. 7c, back on the exponential scale, was 1.083, or about 8% growth per year, and the largest value in Fig. 7d, back on the exponential scale, was 1.146, or about 15% growth per year. These values are similar to published estimates of harbor seal growth rates in natural populations (e.g., Hastings et al., 2012). Fig. 7c,d also clarifies the regional trends, which are difficult to see among the noise in Fig. 2 or by simply filling in the missing sites with predictions (Fig. 7a). For these reasons, smoothing is very popular in disease-mapping applications, but they should be equally attractive for a wide variety of ecological applications. In particular, the XI4RU model (Fig. 7d) is appealing because it uses the data to determine the amount of smoothing. However, we also note

that when used in hierarchical models where, for the data model, the variance is fixed in relation to the mean (e.g., binomial, Bernoulli, and Poisson), the amount of smoothing will be dictated by the assumed variance of the data model. In such cases, we reiterate the discussion on choosing between CAR and IAR.

One practical consideration that is rarely discussed is the case of isolated sites (those with no neighbors) when constructing the neighborhood matrix. Having a row of zeros in  $\mathbf{B}$  in (eqn 2), or in  $\mathbf{C}$  in (eqn 3), will cause problems. It is even easier to see that we cannot divide by zero in (eqn 9), or during row-standardization. Instead, we suggest that the covariance matrix be constructed as

$$\begin{pmatrix} \sigma_I^2 \mathbf{I} & \mathbf{0} \\ \mathbf{0} & \mathbf{\Sigma} \end{pmatrix},$$

where we show the data ordered such that all isolated sites are first, and their corresponding covariance matrix is  $\sigma_I^2 \mathbf{I}$ . The matrix  $\mathbf{\Sigma}$  is the CAR or SAR covariance matrix for the sites connected by neighbors. Note that one of the main issues here is the separation of the variance parameters,  $\sigma_I^2$  and, e.g.,  $\sigma_Z^2$  in (eqn 2) and (eqn 3). As seen in (eqn 9), the autoregressive variance is often scaled by the number of neighbors, and because the isolated sites have no neighbors, it is prudent to give them their own variance parameter.

Our final take-home message concerns software. Does the software check the weights to ensure the covariance matrix will be proper? It may be computationally expensive to check it internally, which lessens the appeal of the autoregressive models, and the software may trust the user to give it a valid weights matrix. Does the software use row-standardization internally? How does the software handle isolated sites? These are some special issues that only pertain to CAR and SAR models, so we suggest investigation of these issues so that the software output can be better understood.

In closing, we note that “networks,” and network models, are increasing throughout science, including ecology (Borrett et al., 2014). Looking again at Fig. 3, if we remove the polygon boundaries, these are network models. Spatial information, in the way of neighborhoods, was used to create the networks. Thus, more general concepts for CAR and SAR models are the graphical

models (Lauritzen, 1996; Whittaker, 2009). A better understanding of these models will lead to their application as network models when data are collected at the nodes of the network, and they can be extended beyond spatial data. This provides a rich area for further model development and research that can include, modify, and enhance the autoregressive models.

## Acknowledgments

The project received financial support from the National Marine Fisheries Service, NOAA. Aerial surveys were authorized under a Marine Mammal Protection Act General Authorization (LOC No. 14590) issued to NMML. The findings and conclusions in the paper are those of the author(s) and do not necessarily represent the views of the reviewers nor the National Marine Fisheries Service, NOAA. Any use of trade, product, or firm names does not imply an endorsement by the US Government.

## Data and Code Accessibility

An R package called spAREco was created that contains all data and code. This document was created using knitr, and the manuscript combining latex and R code is also included in the package. The package can be downloaded at <https://github.com/jayverhoef/SpAREco.git>, with instructions for installing the package.

## References

- Aarts, G., Fieberg, J., Brasseur, S., and Matthiopoulos, J. (2013), “Quantifying the effect of habitat availability on species distributions,” *Journal of Animal Ecology*, 82, 1135–1145.
- Akaike, H. (1973), “Information Theory and an Extension of the Maximum Likelihood Principle,” in *Second International Symposium on Information Theory*, eds. Petrov, B. and Csaki, F., Budapest: Akademiai Kiado, pp. 267–281.

- 704 Anselin, L. (1988), *Spatial Econometrics: Methods and Models*, Dordrecht, the Netherlands: Kluwer  
705 Academic Publishers.
- 706 Banerjee, S., Carlin, B. P., and Gelfand, A. E. (2004), *Hierarchical Modeling and Analysis for*  
707 *Spatial Data*, Boca Raton, FL, USA: Chapman and Hall/CRC.
- 708 Beguería, S. and Pueyo, Y. (2009), “A comparison of simultaneous autoregressive and generalized  
709 least squares models for dealing with spatial autocorrelation,” *Global Ecology and Biogeography*,  
710 18, 273–279.
- 711 Besag, J. (1974), “Spatial Interaction and the Statistical Analysis of Lattice Systems (with discus-  
712 sion),” *Journal of the Royal Statistical Society, Series B*, 36, 192–236.
- 713 — (1975), “Statistical analysis of non-lattice data,” *The Statistician*, 179–195.
- 714 Besag, J. and Kooperberg, C. (1995), “On conditional and intrinsic autoregressions,” *Biometrika*,  
715 82, 733–746.
- 716 Best, N., Cockings, S., Bennett, J., Wakefield, J., and Elliott, P. (2001), “Ecological regression  
717 analysis of environmental benzene exposure and childhood leukaemia: sensitivity to data inac-  
718 curacies, geographical scale and ecological bias,” *Journal of the Royal Statistical Society. Series*  
719 *A (Statistics in Society)*, 164, 155–174.
- 720 Bivand, R. and Piras, G. (2015), “Comparing Implementations of Estimation Methods for Spatial  
721 Econometrics,” *Journal of Statistical Software*, 63, 1–36.
- 722 Borrett, S. R., Moody, J., and Edelman, A. (2014), “The Rise of Network Ecology: Maps of the  
723 topic diversity and scientific collaboration,” *Ecological Modelling*, 293, 111–127.
- 724 Box, G. E. P. and Cox, D. R. (1964), “An Analysis of Transformations,” *Journal of the Royal*  
725 *Statistical Society, Series B*, 26, 211–252.
- 726 Broms, K. M., Johnson, D. S., Altwegg, R., and Conquest, L. L. (2014), “Spatial occupancy  
727 models applied to atlas data show Southern Ground Hornbills strongly depend on protected  
728 areas,” *Ecological Applications*, 24, 363–374.

- Brook, D. (1964), “On the distinction between the conditional probability and the joint probability approaches in the specification of nearest-neighbour systems,” *Biometrika*, 481–483.
- Burnham, K. P. and Anderson, D. R. (2002), *Model Selection and Multimodel Inference: A Practical Information-Theoretic Approach*, New York: Springer-Verlag Inc.
- Chiles, J.-P. and Delfiner, P. (1999), *Geostatistics: Modeling Spatial Uncertainty*, New York: John Wiley & Sons.
- Clayton, D. and Kaldor, J. (1987), “Empirical Bayes estimates of age-standardized relative risks for use in disease mapping,” *Biometrics*, 43, 671–681.
- Clifford, P. (1990), “Markov random fields in statistics,” in *Disorder in Physical Systems: A Volume in Honour of John M. Hammersley*, eds. Grimmett, R. G. and Welsh, D. J. A., New York, NY, USA: Oxford University Press, pp. 19–32.
- Cressie, N. (1990), “The Origins of Kriging,” *Mathematical Geology*, 22, 239–252.
- Cressie, N., Calder, K. A., Clark, J. S., Ver Hoef, J. M., and Wikle, C. K. (2009), “Accounting for Uncertainty in Ecological Analysis: The Strengths and Limitations of Hierarchical Statistical Modeling,” *Ecological Applications*, 19, 553–570.
- Cressie, N. and Wikle, C. K. (2011), *Statistics for Spatio-temporal Data*, Hoboken, New Jersey: John Wiley & Sons.
- Cressie, N. A. C. (1993), *Statistics for Spatial Data, Revised Edition*, New York: John Wiley & Sons.
- Curriero, F. C. (2006), “On the use of non-Euclidean distance measures in geostatistics,” *Mathematical Geology*, 38, 907–926.
- Dormann, C. F., McPherson, J. M., Araújo, M. B., Bivand, R., Bolliger, J., Carl, G., Davies, R. G., Hirzel, A., Jetz, W., Kissling, W. D., Kühn, I., Ohlemüller, R., Peres-Neto, P. R., Reineking, B., Schröder, B., Schurr, F. M., and Wilson, R. (2007), “Methods to account for spatial autocorrelation in the analysis of species distributional data: a review,” *Ecography*, 30, 609–628.

- Earnest, A., Morgan, G., Mengersen, K., Ryan, L., Summerhayes, R., and Beard, J. (2007),  
 “Evaluating the effect of neighbourhood weight matrices on smoothing properties of Condi-  
 tional Autoregressive (CAR) models,” *International Journal of Health Geographics*, 6, 54, doi =  
 10.1016/j.csda.2011.10.022.
- Fay, R. E. and Herriot, R. A. (1979), “Estimates of income for small places: an application of  
 James-Stein procedures to census data,” *Journal of the American Statistical Association*, 74,  
 269–277.
- Gardner, C. L., Lawler, J. P., Ver Hoef, J. M., Magoun, A. J., and Kellie, K. A. (2010),  
 “Coarse-Scale Distribution Surveys and Occurrence Probability Modeling for Wolverine in Inte-  
 rior Alaska,” *The Journal of Wildlife Management*, 74, 1894–1903.
- Gelfand, A. E., Schmidt, A. M., Wu, S., Silander, J. A., Latimer, A., and Rebelo, A. G. (2005),  
 “Modelling species diversity through species level hierarchical modelling,” *Journal of the Royal  
 Statistical Society: Series C (Applied Statistics)*, 54, 1–20.
- Gelfand, A. E. and Smith, A. F. M. (1990), “Sampling-based approaches to calculating marginal  
 densities,” *Journal of the American Statistical Association*, 85, 398–409.
- Haas, S. E., Hooten, M. B., Rizzo, D. M., and Meentemeyer, R. K. (2011), “Forest species diversity  
 reduces disease risk in a generalist plant pathogen invasion,” *Ecology Letters*, 14, 1108–1116.
- Haining, R. (1990), *Spatial Data Analysis in the Social and Environmental Sciences*, Cambridge,  
 UK: Cambridge University Press.
- Hamilton, J. D. (1994), *Time Series Analysis*, vol. 2, Princeton, NJ, USA: Princeton University  
 Press.
- Hammersley, J. M. and Clifford, P. (1971), “Markov fields on finite graphs and lattices,” Unpub-  
 lished Manuscript.
- Hanks, E. M. and Hooten, M. B. (2013), “Circuit theory and model-based inference for landscape  
 connectivity,” *Journal of the American Statistical Association*, 108, 22–33.



779 Harville, D. A. (1997), *Matrix Algebra from a Statistician's Perspective*, New York, NY: Springer.

780 Hastings, K. K., Small, R. J., and Pendleton, G. W. (2012), "Sex-and age-specific survival of harbor  
781 seals (*Phoca vitulina*) from Tugidak Island, Alaska," *Journal of Mammalogy*, 93, 1368–1379.

782 Hooten, M. and Hobbs, N. (2015), "A guide to Bayesian model selection for ecologists," *Ecological*  
783 *Monographs*, 85, 3–28.

784 Huijbregts, C. and Matheron, G. (1971), "Universal kriging (an optimal method for estimating  
785 and contouring in trend surface analysis)," in *Proceedings of Ninth International Symposium on*  
786 *Techniques for Decision-making in the Mineral Industry*, ed. McGerrigle, J. I., The Canadian  
787 Institute of Mining and Metallurgy, Special Volume 12, pp. 159–169.

788 Illian, J. B., Martino, S., Sørbye, S. H., Gallego-Fernández, J. B., Zunzunegui, M., Esquivias, M. P.,  
789 and Travis, J. M. (2013), "Fitting complex ecological point process models with integrated nested  
790 Laplace approximation," *Methods in Ecology and Evolution*, 4, 305–315.

791 Johnson, D. S., Conn, P. B., Hooten, M. B., Ray, J. C., and Pond, B. A. (2013), "Spatial occupancy  
792 models for large data sets," *Ecology*, 94, 801–808.

793 Keitt, T. H., Bjørnstad, O. N., Dixon, P. M., and Citron-Pousty, S. (2002), "Accounting for spatial  
794 pattern when modeling organism-environment interactions," *Ecography*, 25, 616–625.

795 Kissling, W. D. and Carl, G. (2008), "Spatial autocorrelation and the selection of simultaneous  
796 autoregressive models," *Global Ecology and Biogeography*, 17, 59–71.

797 Latimer, A. M., Wu, S., Gelfand, A. E., and Silander Jr, J. A. (2006), "Building statistical models  
798 to analyze species distributions," *Ecological Applications*, 16, 33–50.

799 Lauritzen, S. L. (1996), *Graphical Models*, Oxford, UK: Oxford University Press.

800 Lawson, A. B. (2013), *Bayesian Disease Mapping: Hierarchical Modeling in Spatial Epidemiology*,  
801 Boca Raton, FL: CRC Press.

802 Leroux, B. G., Lei, X., and Breslow, N. (2000), “Estimation of disease rates in small areas: A new  
803 mixed model for spatial dependence,” in *Statistical Models in Epidemiology, the Environment,  
804 and Clinical Trials*, eds. Halloran, M. E. and Berry, D. A., Springer, pp. 179–191.

805 Lunn, D. J., Thomas, A., Best, N., and Spiegelhalter, D. (2000), “WinBUGS-a Bayesian modelling  
806 framework: concepts, structure, and extensibility,” *Statistics and computing*, 10, 325–337.

807 Magoun, A. J., Ray, J. C., Johnson, D. S., Valkenburg, P., Dawson, F. N., and Bowman, J. (2007),  
808 “Modeling wolverine occurrence using aerial surveys of tracks in snow,” *Journal of Wildlife  
809 Management*, 71, 2221–2229.

810 Pace, R. K. and Barry, R. (1997a), “Fast spatial estimation,” *Applied Economics Letters*, 4, 337–  
811 341.

812 — (1997b), “Sparse spatial autoregressions,” *Statistics & Probability Letters*, 33, 291–297.

813 Poley, L. G., Pond, B. A., Schaefer, J. A., Brown, G. S., Ray, J. C., and Johnson, D. S. (2014),  
814 “Occupancy patterns of large mammals in the Far North of Ontario under imperfect detection  
815 and spatial autocorrelation,” *Journal of Biogeography*, 41, 122–132.

816 R Core Team (2014), *R: A Language and Environment for Statistical Computing*, R Foundation  
817 for Statistical Computing, Vienna, Austria.

818 Rue, H. and Held, L. (2005), *Gauss Markov Random Fields: Theory and Applications*, Boca Raton,  
819 FL, USA: Chapman and Hall/CRC.

820 Rue, H., Martino, S., and Chopin, N. (2009), “Approximate Bayesian inference for latent Gaussian  
821 models by using integrated nested Laplace approximations,” *Journal of the Royal Statistical  
822 Society: Series B (Statistical Methodology)*, 71, 319–392.

823 Schabenberger, O. and Gotway, C. A. (2005), *Statistical Methods for Spatial Data Analysis*, Boca  
824 Raton, Florida: Chapman Hall/CRC.

825 Schwarz, G. (1978), “Estimating the Dimension of a Model,” *The Annals of Statistics*, 6, 461–464.

- 826 Shepard, D. (1968), “A two-dimensional interpolation function for irregularly-spaced data,” in  
827 *Proceedings of the 1968 23rd ACM National Conference*, ACM, pp. 517–524.
- 828 Snedecor, G. W. and Cochran, W. G. (1980), *Statistical Methods, Seventh Edition*, Iowa State  
829 University.
- 830 Ver Hoef, J. M., Cameron, M. F., Boveng, P. L., London, J. M., and Moreland, E. E. (2014), “A  
831 spatial hierarchical model for abundance of three ice-associated seal species in the eastern Bering  
832 Sea,” *Statistical Methodology*, 17, 46–66.
- 833 Ver Hoef, J. M. and Jansen, J. K. (2007), “Space-time Zero-inflated Count Models of Harbor Seals,”  
834 *EnvironMetrics*, 18, 697–712.
- 835 Ver Hoef, J. M. and Peterson, E. (2010), “A Moving Average Approach for Spatial Statistical  
836 Models of Stream Networks (with discussion),” *Journal of the American Statistical Association*,  
837 105, 6–18.
- 838 Ver Hoef, J. M., Peterson, E. E., and Theobald, D. (2006), “Spatial Statistical Models That Use  
839 Flow and Stream Distance,” *Environmental and Ecological Statistics*, 13, 449–464.
- 840 Wall, M. M. (2004), “A close look at the spatial structure implied by the CAR and SAR models,”  
841 *Journal of Statistical Planning and Inference*, 121, 311–324.
- 842 Waller, L. A. and Gotway, C. A. (2004), *Applied Spatial Statistics for Public Health Data*, John  
843 Wiley and Sons, New Jersey.
- 844 Whittaker, J. (2009), *Graphical Models in Applied Multivariate Statistics*, Chichester, UK: Wiley  
845 Publishing.
- 846 Whittle, P. (1954), “On stationary processes in the plane,” *Biometrika*, 41, 434–449.

Table 1: Common objectives when using spatial autoregressive models. Notation for the model components comes from (eqn 12).

Objective	Description	Example Literature	Model Component
1. Model Comparison & Selection	CAR and SAR models are often part of a spatial (generalized) linear model. One goal, prior to further inference, might be to compare models, and then choose one. The choice of the form of a CAR or SAR model may be important in this comparison and selection.	Hooten and Hobbs (2015)	$L(\mathbf{y} \cdot)$
2. Regression	The goal is to estimate the spatial regression coefficients, which quantify how an explanatory variable “affects” the response variable.	Clayton and Kaldor (1987)	$\beta$
3. Autocorrelation	The goal is to estimate the “strength” of autocorrelation, especially if it represents an ecological idea such as spatial connectivity, which quantifies how similarly sites change in the residual errors, after accounting for regression effects.	Gardner et al. (2010)	$\rho$
4. Neighborhood Structure	The goal is to estimate covariate effects on neighborhood structure. Although rarely used, covariates can be included in the precision matrix to see how they affect neighborhood structure; e.g., causing more or less correlation.	Hanks and Hooten (2013)	$\theta$
5. Prediction	This is the classical goal of geostatistics, and is rarely used in CAR and SAR models. However, if sites have missing data, prediction is possible.	Gardner et al. (2010)	$\mathbf{y}_u$ and/or $\mu_u$
6. Smoothing	The goal is to create values at spatial sites that smooth over observed data by using values from nearby locations to provide better estimates.	Clayton and Kaldor (1987)	$g(\mu)$

Table 2: A variety of candidate models used to explore spatial autoregressive models for the example data set. For fixed effects, the **1** indicates an overall mean in the model, and  $\mathbf{X}_{\text{stock}}$  includes an additional categorical effect for each stock. A  $[\cdot]_+$  around a matrix indicates row-standardization, and for CAR models,  $[\mathbf{M}]_+$  is the appropriate diagonal matrix for such row standardization. The matrices themselves are described in the text. For model codes, m indicates an overall mean only, whereas X indicates the additional stock effect in the fixed effects. A C indicates a CAR model, an S a SAR model, and an I an IAR model. A 1 indicates a first-order neighborhood, a 2 a second-order neighborhood, and a 4 a fourth-order neighborhood. An R indicates row-standardization. A D indicates inclusion of Euclidean distance within neighborhoods, and S a cross stock connectivity matrix. A U at the end indicates inclusion of an additive random effect of uncorrelated variables.

Model Code	Fixed Effects	Covariance Model	No. Parms
mU	<b>1</b>	$\sigma_\varepsilon^2 \mathbf{I}$	2
mC1R	<b>1</b>	$\sigma_Z^2 (\mathbf{I} - \rho [\mathbf{W}_1]_+)^{-1} [\mathbf{M}]_+$	3
XU	$\mathbf{X}_{\text{stock}}$	$\sigma_\varepsilon^2 \mathbf{I}$	6
XC1R	$\mathbf{X}_{\text{stock}}$	$\sigma_Z^2 (\mathbf{I} - \rho [\mathbf{W}_1]_+)^{-1} [\mathbf{M}]_+$	7
XC1	$\mathbf{X}_{\text{stock}}$	$\sigma_Z^2 (\mathbf{I} - \rho \mathbf{W}_1)^{-1}$	7
XS1R	$\mathbf{X}_{\text{stock}}$	$\sigma_Z^2 [(\mathbf{I} - \rho [\mathbf{W}_1]_+)(\mathbf{I} - \rho [\mathbf{W}_1]_+)]^{-1}$	7
XS1	$\mathbf{X}_{\text{stock}}$	$\sigma_Z^2 [(\mathbf{I} - \rho \mathbf{W}_1)(\mathbf{I} - \rho \mathbf{W}_1)]^{-1}$	7
XC2R	$\mathbf{X}_{\text{stock}}$	$\sigma_Z^2 (\mathbf{I} - \rho [\mathbf{W}_2]_+)^{-1} [\mathbf{M}]_+$	7
XC4R	$\mathbf{X}_{\text{stock}}$	$\sigma_Z^2 (\mathbf{I} - \rho [\mathbf{W}_4]_+)^{-1} [\mathbf{M}]_+$	7
XC4	$\mathbf{X}_{\text{stock}}$	$\sigma_Z^2 (\mathbf{I} - \rho \mathbf{W}_4)^{-1}$	7
XI4RU	$\mathbf{X}_{\text{stock}}$	$(\text{NA, eqn 9}) + \varepsilon^2 \mathbf{I}$	7
XC4RD	$\mathbf{X}_{\text{stock}}$	$\sigma_Z^2 (\mathbf{I} - \rho [\mathbf{W}_4 \odot \exp(-\mathbf{D}/\theta_2)]_+)^{-1} [\mathbf{M}]_+$	8
XC4RDS	$\mathbf{X}_{\text{stock}}$	$\sigma_Z^2 (\mathbf{I} - \rho [\mathbf{W}_4 \odot \exp(-\mathbf{D}/\theta_2) \odot \exp(-\mathbf{S}/\theta_2)]_+)^{-1} [\mathbf{M}]_+$	9
XC4RDU	$\mathbf{X}_{\text{stock}}$	$\sigma_Z^2 (\mathbf{I} - \rho [\mathbf{W}_4 \odot \exp(-\mathbf{D}/\theta_2)]_+)^{-1} [\mathbf{M}]_+ + \sigma_\varepsilon^2 \mathbf{I}$	9

Table 3: Estimated fixed effects for several models listed in Table 2. Both the estimate (Est.) and estimated standard error (Std.Err.) are given for each model. All models use maximum likelihood estimates (MLE), except for XC4R model, we distinguish the MLE estimate with -mle, and a Bayesian estimate using Markov chain Monte Carlo with -mcmc.

Parameter	XU		XC4R-mle		XC4R-mcmc		XC4RD	
	Est.	Std.Err.	Est.	Std.Err.	Est.	Std.Err.	Est.	Std.Err.
$\mu$	-0.079	0.0225	-0.080	0.0288	-0.082	0.0330	-0.077	0.0290
$\beta_{\text{stock } 2}$	0.048	0.0298	0.063	0.0379	0.063	0.0429	0.058	0.0386
$\beta_{\text{stock } 3}$	0.093	0.0281	0.095	0.0355	0.097	0.0386	0.092	0.0356
$\beta_{\text{stock } 4}$	0.132	0.0279	0.135	0.0346	0.138	0.0406	0.132	0.0346
$\beta_{\text{stock } 5}$	0.084	0.0259	0.093	0.0327	0.096	0.0378	0.089	0.0330

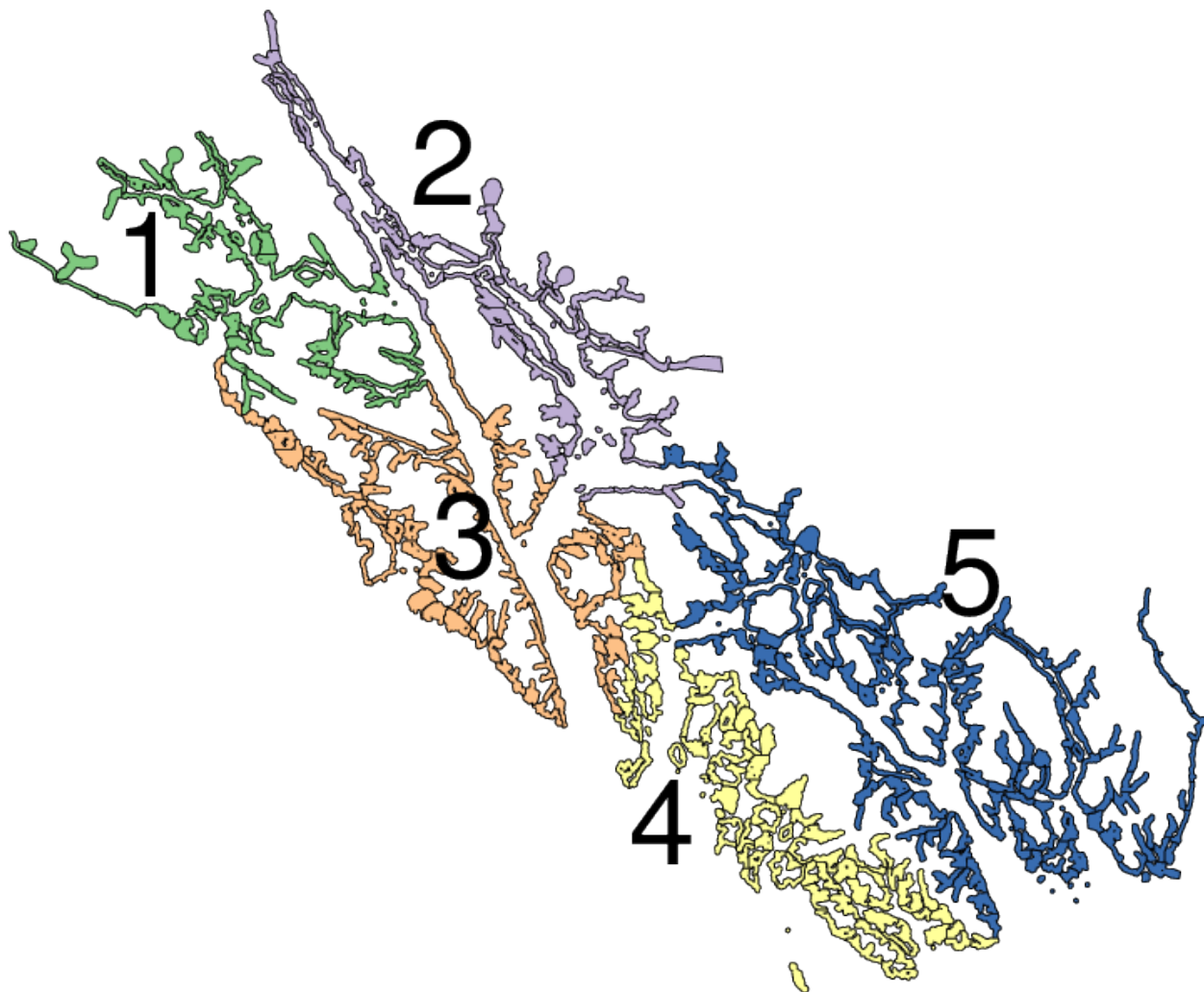


Figure 1: Study area in Southeast Alaska. Survey polygons were established around the coast of the mainland and all islands, which were surveyed for harbor seals. The study area comprises 5 stocks, each with their own color, and are numbered for further reference.

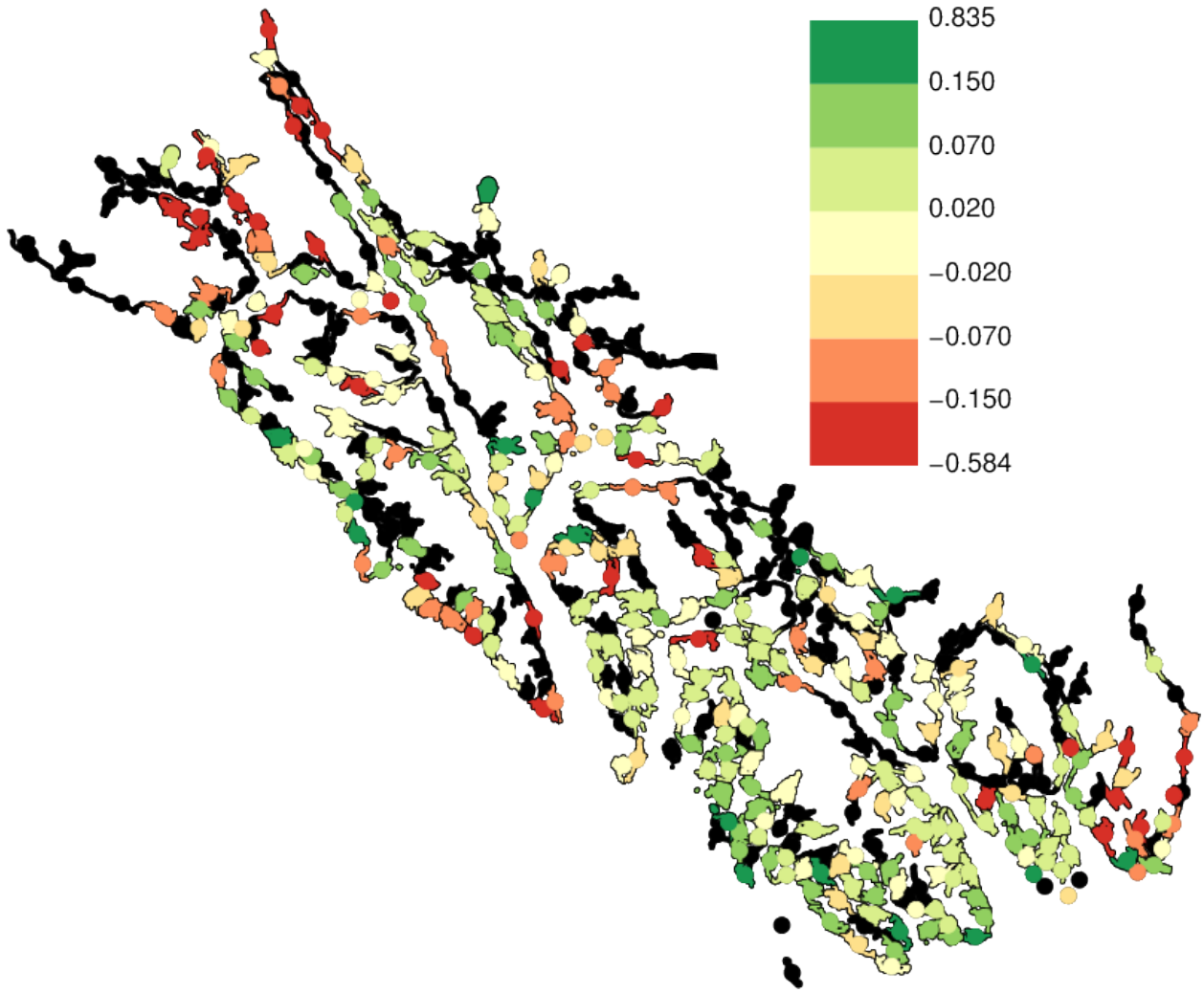


Figure 2: Map of the raw data, where polygons are colored by their trend values. The black polygons have missing data. Because some polygons were small and it was difficult to see colors in them, all polygons were also overwritten by a circle of the same color. The trend values were categorized by colors, with increasing trends in green, and decreasing trends in red, with the cutoff values given by the color ramp.

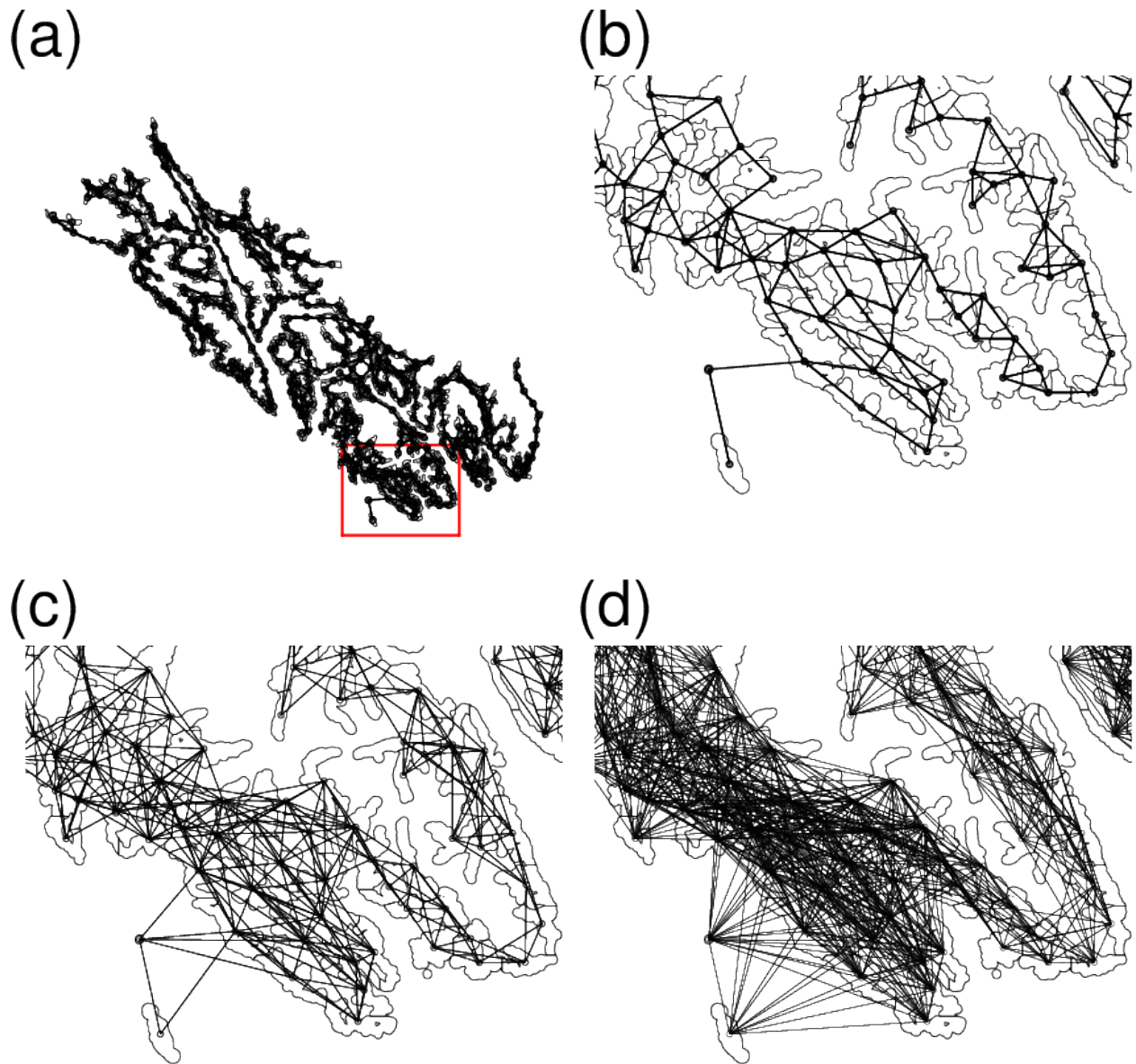


Figure 3: First, second, and fourth-order neighbor definitions for the survey polygons. (a) First-order neighbors for all polygons. The red rectangle is the area for a closer view in the following subfigures: (b) first-order neighbors; (c) second-order neighbors; and (d) fourth-order neighbors.



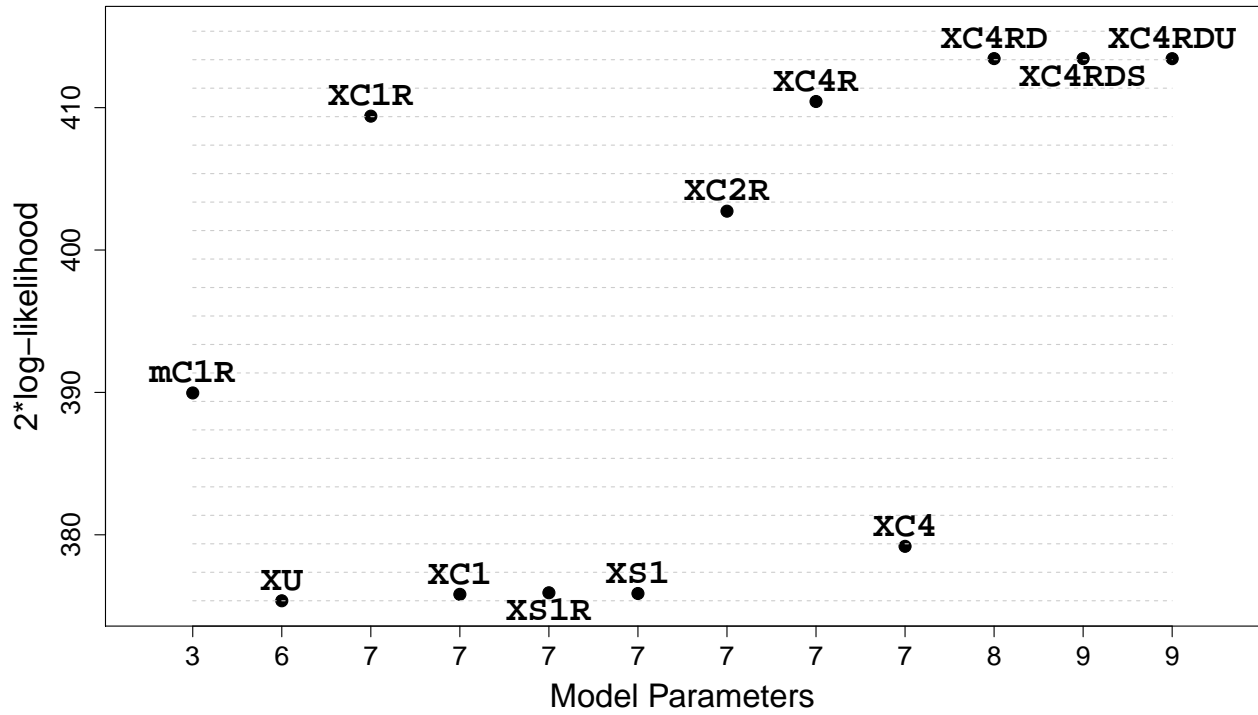


Figure 4: Two times the log-likelihood for the optimized (maximized) fit for the models given in Table 2. Model mU had a much lower value (350.2) and is not shown. Starting with model XU, the dashed grey lines show increments of 2, which helps evaluate the relative importance of models by either an AIC or a likelihood-ratio test criteria.

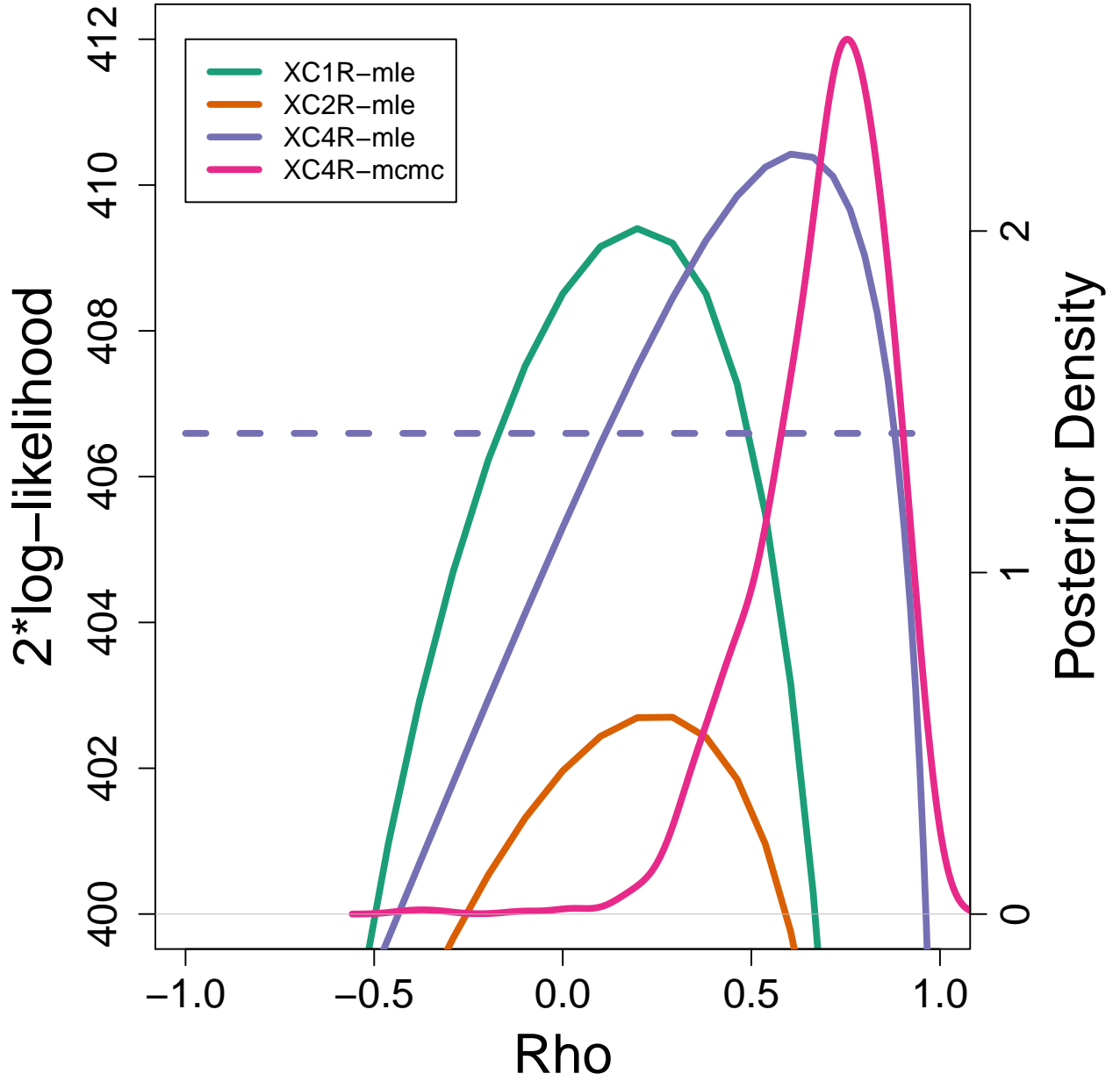


Figure 5: The different colored solid lines show 2Log-likelihood profiles of  $\rho$  for three different models, listed in the legend. If the model is followed by -mle, then the maximum of the profile provides the maximum likelihood estimate, and the 2log-likelihood is given by the left y-axis, while if it is followed by -mcmc, then it is the posterior distribution from a Bayesian model with a uniform prior on  $\rho$ , and the density is given by the right y-axis. The horizontal dashed line is the maximum value for XC4R minus 3.841, the 0.05  $\alpha$ -level value of a chi-squared distribution on one degree of freedom.

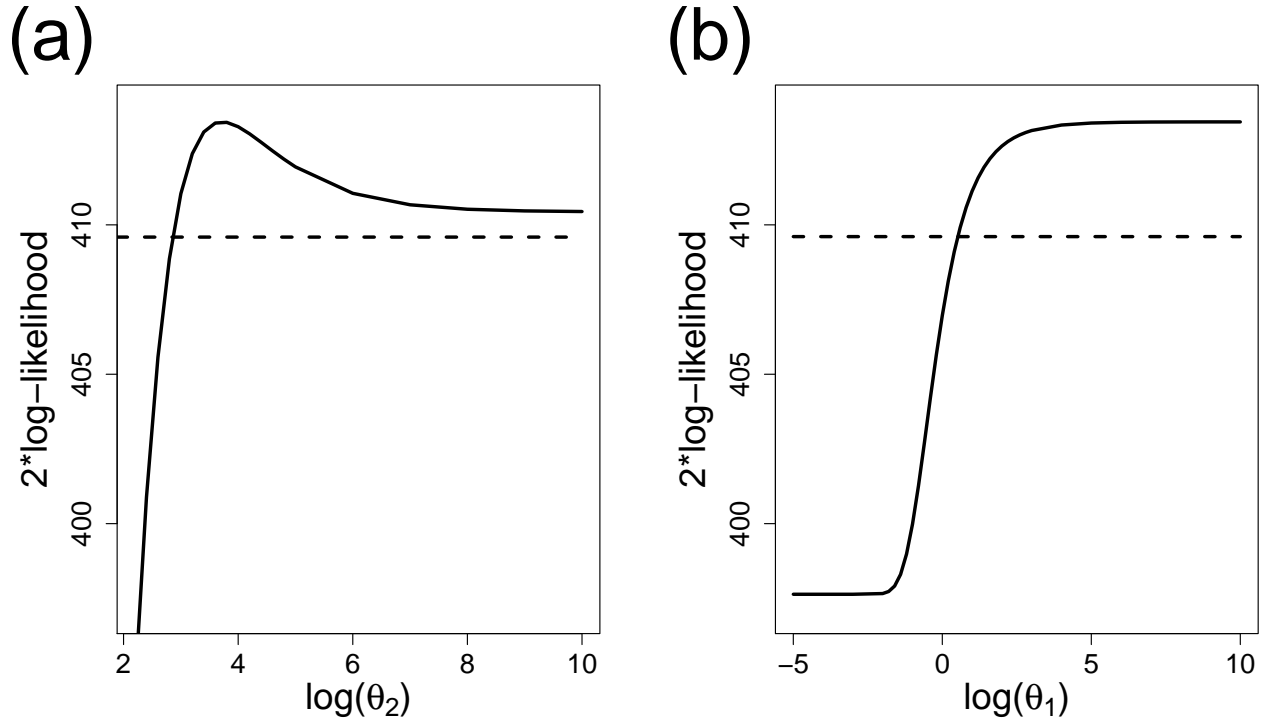


Figure 6: A) The solid line is the 2Log-likelihood profile of  $\theta_2$  for model XC4RD. B) The solid line is the 2Log-likelihood profile of  $\theta_1$  for model XC4RDS. For each figure, the horizontal dashed line is the maximum value for the model minus 3.841, the 0.05  $\alpha$ -level value of a chi-squared distribution on one degree of freedom.

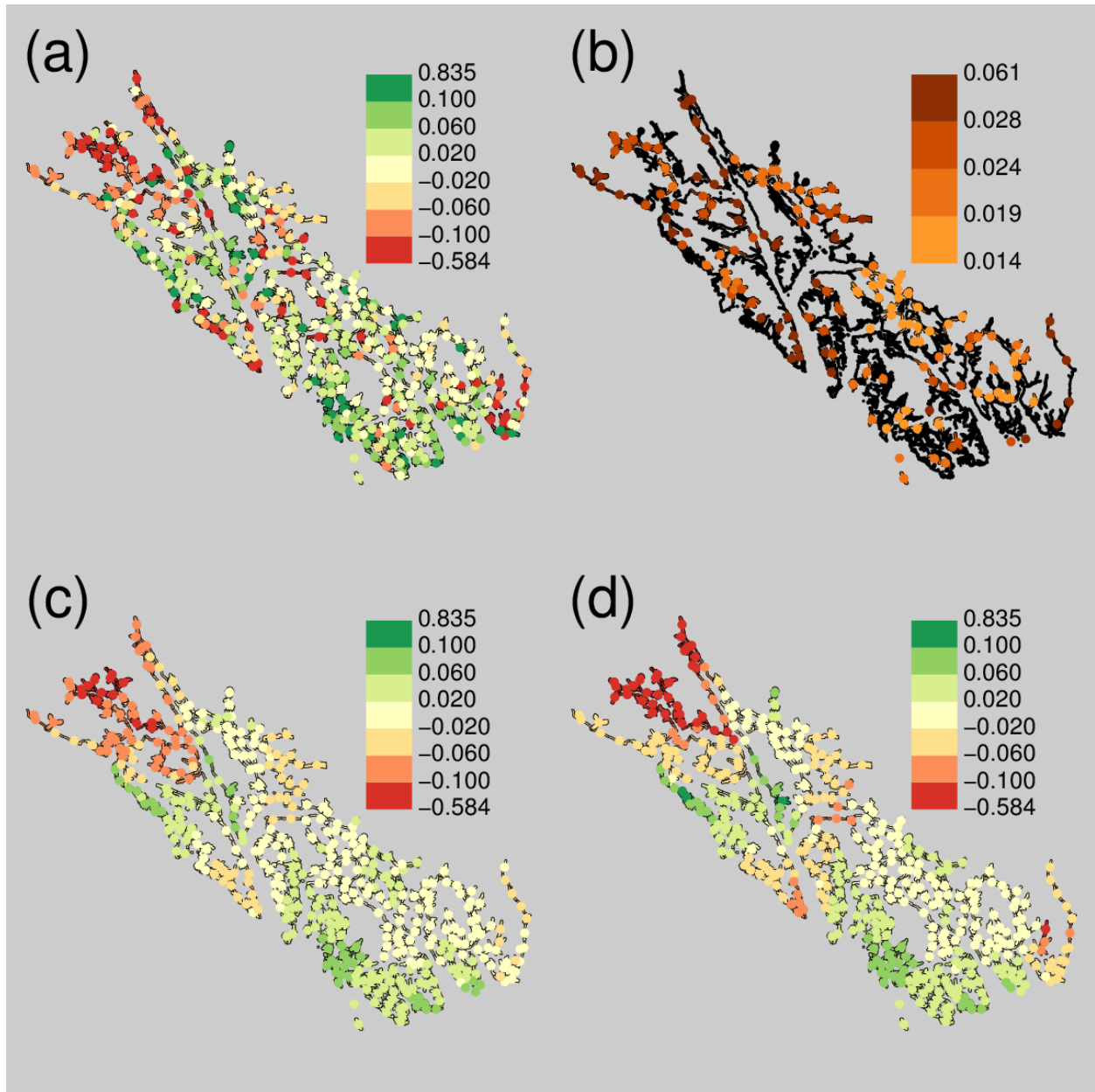


Figure 7: Predictions and smoothing for the stock trend data. (a) Predictions, using universal kriging from the XC4R model, at unsampled locations have been added to the raw observed data from sampled locations. (b) Prediction standard errors for unsampled locations using universal kriging from the XC4R. (c) Smoothing over all locations using conditional expectation based on the XC4R model. (d) Smoothing over all locations by using posterior predictions (mean of posterior distributions) using the XI4RU model in a Bayesian hierarchical model.

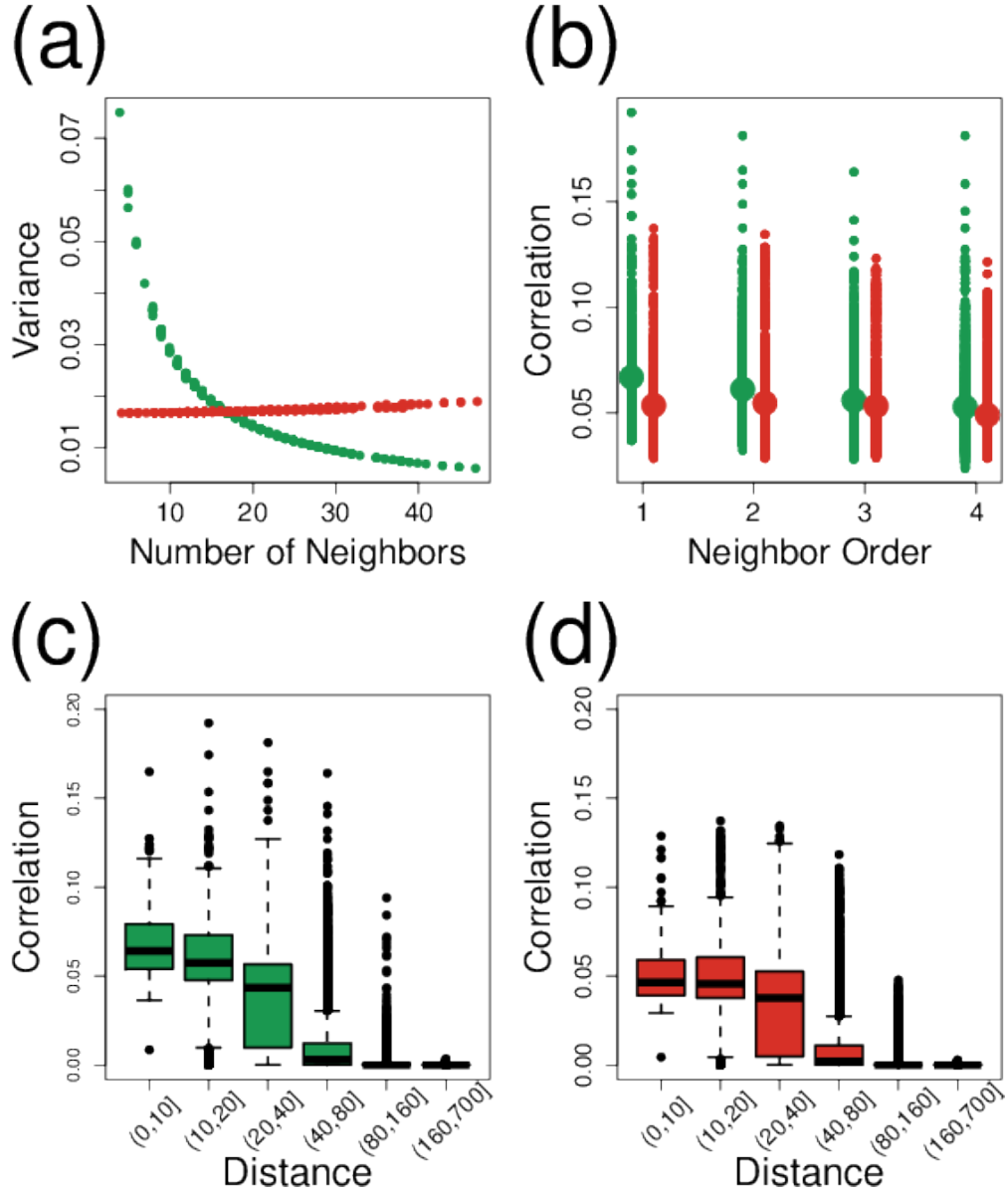


Figure 8: For all subfigures, red is used for model XC4 and green is used for the same model, XC4R, but with row-standardization. A) Marginal variances of the multivariate covariance matrix (diagonal elements of  $\Sigma$ ) as a function of the numbers of neighbors. B) All pairwise correlations as a function of the neighborhood order between sites. The larger circle is the average value. C) and D) Boxplots of pairwise correlation as a function of distance between polygon centroids, binned into classes, for models XC4R and XC4, respectively.

# 1 APPENDIX A: Errors in the Literature

The fact that CAR and SAR models are developed for the precision matrix, in contrast to geostatistical models being developed for the covariance matrix, has caused some confusion in the ecological literature. For example, in comparing geostatistical models to SAR models, Beguería and Pueyo (2009) state “Semivariogram models account for spatial autocorrelation *at all possible distance lags*, and thus they do not require a priori specification of the window size and the covariance structure,” (emphasis by the original authors). CAR and SAR models also account for spatial autocorrelation at all possible lags, as seen in Fig 8c,d). In a temporal analogy, the autoregressive AR1 time series models also account for autocorrelation at all possible lags, where the conditional specification  $Z_{i+1} = \phi Z_i + \nu_i$ , with  $\nu_i$  an independent random shock and  $|\phi| < 1$ , implies that  $\text{corr}(Z_i, Z_{i+t}) = \phi^t$  for all  $t$ . In fact, if we restrict  $0 < \phi < 1$ , then this can be reparameterized as  $\text{corr}(Z_i, Z_{i+t}) = \exp(-t(-\log(\phi)))$ , which is an exponential geostatistical model with range parameter  $-\log(\phi)$ . While there are interesting results in Beguería and Pueyo (2009), a restriction on the range of autocorrelation is not a reason that CAR/SAR models might perform poorly against a geostatistical model. The important concept is that the autoregressive specification is local in the precision matrix and not in the covariance matrix.

CAR models are often incorrectly characterized. For example, Keitt et al. (2002) characterize CAR models as:  $\mathbf{Y} = \mathbf{X}\boldsymbol{\beta} + \rho\mathbf{C}(\mathbf{Y} - \mathbf{X}\boldsymbol{\beta}) + \boldsymbol{\varepsilon}$ , with a stated covariance matrix of  $\sigma^2(\mathbf{I} - \rho\mathbf{C})^{-1}$ , where  $\mathbf{C}$  is symmetric. While we believe their implementation may have been correct, and there are excellent and important results in Keitt et al. (2002), their construction leads to a SAR covariance matrix of  $\sigma^2(\mathbf{I} - \rho\mathbf{C})^{-1}(\mathbf{I} - \rho\mathbf{C})^{-1}$  if  $\text{var}(\boldsymbol{\varepsilon}) = \sigma^2\mathbf{I}$  and  $\mathbf{C}$  is symmetric. Even to characterize a CAR model as  $\sigma^2(\mathbf{I} - \rho\mathbf{C})^{-1}$  with symmetric  $\mathbf{C}$  is overly restrictive, as we have demonstrated that an asymmetric  $\mathbf{C}$  with the proper  $\mathbf{M}$  will still satisfy (eqn 8), or alternatively that  $\boldsymbol{\Sigma}^{-1} = (\mathbf{M}^{-1} - \mathbf{C})/\sigma^2$ , where  $\mathbf{C}$  is symmetric but  $\mathbf{M}^{-1}$  is not necessarily constant on the diagonals. In fact, constraining a CAR model to  $\sigma^2(\mathbf{I} - \rho\mathbf{C})^{-1}$  does not allow for row-standardized models. These mistakes are perpetuated in (Dormann et al., 2007), and we have seen similar errors in describing CAR models as SAR models in other literature, presentations, and help sites on the internet.

876 Dormann et al. (2007) also claim that any SAR model is a CAR model, which agrees with  
877 the literature (e.g., Cressie, 1993, p. 409), but then they show an incorrect proof (it is also incorrect  
878 in Haining, 1990, p. 89, and likely beginning there), because they do not consider that  $\mathbf{C}$  for a CAR  
879 model must have zeros along the diagonal. In fact we demonstrate in Appendix B that, despite  
880 literature to the contrary, CAR models and SAR models can be written equivalently, and we give  
881 further details.

## 2 APPENDIX B: Equivalence of CAR and SAR Models

To establish when CAR models can be written as SAR, and vice versa, we need the following equality,

$$(\mathbf{I} - \mathbf{C})^{-1}\mathbf{M} = (\mathbf{I} - \mathbf{B})^{-1}\mathbf{\Lambda}(\mathbf{I} - \mathbf{B}')^{-1}, \quad \text{B.1}$$

satisfying, for the CAR covariance matrix on the left-hand side, 1)  $(\mathbf{I} - \mathbf{C})^{-1}$  exists, 2)  $c_{ii} = 0 \forall i$ , and 3)  $c_{ij}/m_{ii} = c_{ji}/m_{jj} \forall i, j$ ; and for the SAR covariance matrix on the right-hand side, 4)  $(\mathbf{I} - \mathbf{B})^{-1}$  exists, and 5)  $b_{ii} = 0 \forall i$ . Notice that we write the SAR covariance matrix as  $(\mathbf{I} - \mathbf{B})^{-1}\mathbf{\Lambda}(\mathbf{I} - \mathbf{B}')^{-1}$ , where  $\mathbf{\Lambda}$  is a diagonal matrix, in (B.1), following Cressie (1993, p. 409), which is a little more general than the SAR covariance matrix given in (eqn 2). Ultimately, this demonstration relies on establishing that any zero-mean Gaussian distribution on a finite set of points,  $\mathbf{Z} \sim N(\mathbf{0}, \mathbf{\Sigma})$  can be written as either the left-hand side, or the right-hand side of (B.1). Note, we make use of the following result: if  $\mathbf{D}$  is diagonal, and  $\mathbf{Q}$  has zero on the diagonals, then both  $\mathbf{DQ}$  and  $\mathbf{QD}$  have zeros on the diagonal.

First consider obtaining the left-hand side of (B.1); this result is also given by Cressie (1993, p. 434). Write  $\mathbf{\Sigma}^{-1} = \mathbf{D} - \mathbf{Q}$ , where  $\mathbf{D}$  is diagonal and  $\mathbf{Q}$  has zeros on the diagonal. Then factor out  $\mathbf{D}$  so that  $\mathbf{\Sigma}^{-1} = \mathbf{D}(\mathbf{I} - \mathbf{D}^{-1}\mathbf{Q})$ , and now let  $\mathbf{M} = \mathbf{D}^{-1}$  and  $\mathbf{C} = \mathbf{D}^{-1}\mathbf{Q}$ , then  $(\mathbf{I} - \mathbf{C})^{-1}$  exists because  $\mathbf{\Sigma}^{-1}$  and  $\mathbf{D}^{-1}$  exist,  $\mathbf{C}$  will have zeros on the diagonals, and condition 3) is satisfied by construction (because it is the requirement for symmetry). Thus,  $\mathbf{\Sigma}^{-1}$  can be expressed as  $\mathbf{M}^{-1}(\mathbf{I} - \mathbf{C})$  and  $\mathbf{\Sigma} = (\mathbf{I} - \mathbf{C})^{-1}\mathbf{M}$  satisfying conditions 1) to 3).

Next, consider the right-hand side of (B.1). Write  $\mathbf{\Sigma}^{-1} = \mathbf{LL}'$ . An important note is that this is not unique. A Cholesky decomposition satisfies this, where  $\mathbf{L}$  is lower triangular, or a singular value decomposition could be used, where square roots of the eigenvalues are multiplied in the matrix of eigenvectors. In any case, let  $\mathbf{LL}' = (\mathbf{G} - \mathbf{P})(\mathbf{G}' - \mathbf{P}')$ , where  $\mathbf{G}$  is diagonal and  $\mathbf{P}$  has zero diagonals. Then factor out  $\mathbf{G}$  to obtain  $\mathbf{LL}' = (\mathbf{I} - \mathbf{PG}^{-1})\mathbf{GG}(\mathbf{I} - \mathbf{G}^{-1}\mathbf{P}')$ , and now let  $\mathbf{\Lambda}^{-1} = \mathbf{GG}$  and  $\mathbf{B}' = \mathbf{PG}^{-1}$ . Notice that  $(\mathbf{PG}^{-1})' = \mathbf{G}^{-1}\mathbf{P}'$  because  $\mathbf{G}^{-1}$  is diagonal. Moreover,  $(\mathbf{I} - \mathbf{B})^{-1}$  exists because  $\mathbf{L}^{-1}$  and  $\mathbf{G}^{-1}$  exist and  $\mathbf{B}$  will have zeros on the diagonals. Thus,  $\mathbf{\Sigma}^{-1}$  can be expressed as  $(\mathbf{I} - \mathbf{B}')^{-1}\mathbf{\Lambda}^{-1}(\mathbf{I} - \mathbf{B})$  and  $\mathbf{\Sigma} = (\mathbf{I} - \mathbf{B})^{-1}\mathbf{\Lambda}^{-1}(\mathbf{I} - \mathbf{B}')^{-1}$  satisfying conditions



908 4) and 5). Note that in order to write it as  $(\mathbf{I} - \mathbf{B})^{-1}(\mathbf{I} - \mathbf{B}')^{-1}$  we need to find  $\mathbf{L}$  with ones on  
 909 the diagonal.

910 Hence, we have demonstrated that any zero-mean Gaussian distribution on a finite set  
 911 of points,  $\mathbf{Z} \sim N(\mathbf{0}, \mathbf{\Sigma})$  can be written as either the left-hand side, or the right-hand side of  
 912 (B.1), with the important difference that a CAR model is uniquely determined from  $\mathbf{\Sigma}$  but a  
 913 SAR model is not so uniquely determined. That a CAR is unique is easy to see from the algebra  
 914 used to derive it. To see more fully why a SAR model is not uniquely determined, notice that  
 915  $\mathbf{\Sigma}^{-1} = \mathbf{L}\mathbf{L}' = \mathbf{L}(\mathbf{A}'\mathbf{A})\mathbf{L}' = (\mathbf{L}\mathbf{A}')(\mathbf{A}\mathbf{L}') = \mathbf{L}_*\mathbf{L}_*'$ , where the columns of  $\mathbf{A}$  are orthonormal. A SAR  
 916 model can be developed as readily for  $\mathbf{L}_*$  as for  $\mathbf{L}$ . In fact, if we think of  $\mathbf{A}$  as coordinate vectors,  
 917 any rotation of the matrix  $\mathbf{A}$  will create yet another SAR model, so there are an infinite number  
 918 of them.

919 With this appendix, we also wish to correct an error that has been perpetuating in the  
 920 literature, beginning with Haining (1990, p. 89), and we also found it in Schabenberger and Gotway  
 921 (2005) and Dormann et al. (2007). The authors state that, suppose in (B.1) that  $\mathbf{M} = \mathbf{I}$  and  $\mathbf{A} = \mathbf{I}$ ,  
 922 so that  $\mathbf{C}$  is symmetric. That implies that  $(\mathbf{I} - \mathbf{C})^{-1} = [(\mathbf{I} - \mathbf{B})(\mathbf{I} - \mathbf{B}')]^{-1} = (\mathbf{I} - \mathbf{B} - \mathbf{B}' + \mathbf{B}\mathbf{B}')^{-1}$ .  
 923 So, while  $\mathbf{C} = \mathbf{B} + \mathbf{B}' - \mathbf{B}\mathbf{B}'$  is sufficient for equality, it is not necessary, and it lacks a critical  
 924 component; that  $\mathbf{B} + \mathbf{B} - \mathbf{B}\mathbf{B}'$  must have zeros on the diagonal for  $\mathbf{C}$  to be a CAR model. The  
 925 proper way to proceed was outlined above, by letting  $\mathbf{C} = \mathbf{D}^{-1}\mathbf{Q}$  in the equality

$$(\mathbf{I} - \mathbf{D}^{-1}\mathbf{Q})^{-1}\mathbf{D}^{-1} = (\mathbf{I} - \mathbf{B} - \mathbf{B}' + \mathbf{B}\mathbf{B}')^{-1},$$

926 where the left-hand side is uniquely determined from the right-hand size, and  $\mathbf{C}$  satisfies the re-  
 927 quirement for a CAR model. As we demonstrated in the previous paragraph, it is not possible to  
 928 go uniquely from the left-hand side to the right-hand side without additional constraints.

### 3 APPENDIX C: Maximum Likelihood Estimation for CAR/SAR Models with Missing Data

We begin by finding analytical solutions when we can, and then substituting them into the likelihood to reduce the number of parameters as much as possible for the full covariance matrix. Assume a linear model,

$$\mathbf{y} = \mathbf{X}\boldsymbol{\beta} + \boldsymbol{\varepsilon},$$

where  $\mathbf{y}$  is a vector of response variable,  $\mathbf{X}$  is a design matrix of full rank,  $\boldsymbol{\beta}$  is a vector of parameters, and the zero-mean random errors have a multivariate normal distribution,  $\boldsymbol{\varepsilon} \sim N(\mathbf{0}, \boldsymbol{\Sigma})$ , where  $\boldsymbol{\Sigma}$  is a patterned covariance matrix; i.e., it has non-zero off-diagonal elements. Suppose that  $\boldsymbol{\Sigma}$  has parameters  $\{\theta, \boldsymbol{\rho}\}$  and can be written as  $\boldsymbol{\Sigma} = \theta \mathbf{V}_{\boldsymbol{\rho}}$ , where  $\theta$  is an overall variance parameter and  $\boldsymbol{\rho}$  are parameters that structure  $\mathbf{V}_{\boldsymbol{\rho}}$  as a non-diagonal matrix, and we show the dependency as a subscript. Note that  $\boldsymbol{\Sigma}^{-1} = \mathbf{V}_{\boldsymbol{\rho}}^{-1}/\theta$ . Recall that the maximum likelihood estimate of  $\boldsymbol{\beta}$  for any  $\{\theta, \boldsymbol{\rho}\}$  is  $\hat{\boldsymbol{\beta}} = (\mathbf{X}'\mathbf{V}_{\boldsymbol{\rho}}^{-1}\mathbf{X})^{-1}\mathbf{X}'\mathbf{V}_{\boldsymbol{\rho}}^{-1}\mathbf{y}$ . By substituting  $\hat{\boldsymbol{\beta}}$  into the normal likelihood equations,  $-2$  times the loglikelihood for a normal distribution is

$$\mathcal{L}(\theta, \boldsymbol{\rho}|\mathbf{y}) = (\mathbf{y} - \mathbf{X}\hat{\boldsymbol{\beta}})' \boldsymbol{\Sigma}^{-1} (\mathbf{y} - \mathbf{X}\hat{\boldsymbol{\beta}}) + \log(|\boldsymbol{\Sigma}|) + n\log(2\pi),$$

where  $n$  is the length of  $\mathbf{y}$ , but this can be written as,

$$\mathcal{L}(\theta, \boldsymbol{\rho}|\mathbf{y}) = \mathbf{r}_{\boldsymbol{\rho}}' \mathbf{V}_{\boldsymbol{\rho}}^{-1} \mathbf{r}_{\boldsymbol{\rho}} / \theta + n\log(\theta) + \log(|\mathbf{V}|) + n\log(2\pi) \tag{C.1}$$

where  $\mathbf{r}_{\boldsymbol{\rho}} = (\mathbf{y} - \mathbf{X}\hat{\boldsymbol{\beta}})$  (notice that  $\hat{\boldsymbol{\beta}}$  is a function of  $\boldsymbol{\rho}$ , so we show that dependency for  $\mathbf{r}$  as well. Conditioning on  $\boldsymbol{\rho}$  yields

$$\mathcal{L}(\theta|\boldsymbol{\rho}, \mathbf{y}) = \mathbf{r}_{\boldsymbol{\rho}}' \mathbf{V}_{\boldsymbol{\rho}}^{-1} \mathbf{r}_{\boldsymbol{\rho}} / \theta + n\log(\theta) + \text{terms not containing } \theta$$

945 and minimizing for  $\theta$  involves setting

$$\frac{\partial \mathcal{L}(\theta|\boldsymbol{\rho}, \mathbf{y})}{\partial \theta} = -\mathbf{r}'_{\boldsymbol{\rho}} \mathbf{V}_{\boldsymbol{\rho}}^{-1} \mathbf{r}_{\boldsymbol{\rho}} / \theta^2 + n / \theta$$

946 equal to zero, yielding the maximum likelihood estimate

$$\hat{\theta} = \mathbf{r}'_{\boldsymbol{\rho}} \mathbf{V}_{\boldsymbol{\rho}}^{-1} \mathbf{r}_{\boldsymbol{\rho}} / n. \quad \text{C.2}$$

947 Substituting (C.2) back into (C.1) yields the -2loglikelihood as a function of  $\boldsymbol{\rho}$  only,

$$\mathcal{L}(\boldsymbol{\rho}|\mathbf{y}) = n \log(\mathbf{r}'_{\boldsymbol{\rho}} \mathbf{V}_{\boldsymbol{\rho}}^{-1} \mathbf{r}_{\boldsymbol{\rho}}) + \log(|\mathbf{V}_{\boldsymbol{\rho}}|) + n(\log(2\pi) + 1 - \log(n)). \quad \text{C.3}$$

948 Equation (C.3) can be minimized numerically to yield the MLE  $\hat{\boldsymbol{\rho}}$ , and then  $\hat{\theta} = \mathbf{r}'_{\hat{\boldsymbol{\rho}}} \mathbf{V}_{\hat{\boldsymbol{\rho}}}^{-1} \mathbf{r}_{\hat{\boldsymbol{\rho}}} / n$ , and  
 949  $\hat{\boldsymbol{\beta}} = (\mathbf{X}' \mathbf{V}_{\hat{\boldsymbol{\rho}}}^{-1} \mathbf{X})^{-1} \mathbf{X}' \mathbf{V}_{\hat{\boldsymbol{\rho}}}^{-1} \mathbf{y}$ .

950 We developed the inverse covariance matrix  $\boldsymbol{\Sigma}_A^{-1} = \text{diag}(\mathbf{W}\mathbf{1}) - \rho \mathbf{W}$ , and here we use  $\boldsymbol{\Sigma}_A$   
 951 to denote it is for *all* locations, those with observed data as well as those without. Without missing  
 952 data, (C.3) can be evaluated quickly by factoring out an overall variance parameter from  $\boldsymbol{\Sigma}_A^{-1}$   
 953 and using sparse matrix methods to quickly and efficiently evaluate  $|\mathbf{V}_{\boldsymbol{\rho}}|$  by recalling that  $|\mathbf{V}_{\boldsymbol{\rho}}|$   
 954  $= 1/|\mathbf{V}_{\boldsymbol{\rho}}^{-1}|$ . However, when there are missing data, there is no guarantee that  $\mathbf{V}_{\boldsymbol{\rho}}$  will be sparse.  
 955 The obvious and direct approach is to first obtain  $\boldsymbol{\Sigma}_A = (\boldsymbol{\Sigma}_A^{-1})^{-1}$ , and then obtain  $\mathbf{V}_{\boldsymbol{\rho}} = \boldsymbol{\Sigma}[\mathbf{i}, \mathbf{i}]$ ,  
 956 where  $\mathbf{i}$  is a vector of indicators that subsets the rows and columns of  $\boldsymbol{\Sigma}$  to only those for sampled  
 957 locations. Then, a third step is a second inverse to find  $\mathbf{V}_{\boldsymbol{\rho}}^{-1}$ . This is computationally expensive.  
 958 A faster way uses results from partitioned matrices and Schur complements. In general, let the  
 959 square matrix  $\boldsymbol{\Sigma}$  with dimensions  $(m+n) \times (n+m)$  be partitioned into block submatrices,

$$\underset{(m+n) \times (m+n)}{\boldsymbol{\Sigma}} = \begin{bmatrix} \underset{m \times m}{\mathbf{A}} & \underset{m \times n}{\mathbf{B}} \\ \underset{n \times m}{\mathbf{C}} & \underset{n \times n}{\mathbf{D}} \end{bmatrix}$$

960 with dimensions given below each matrix. Assume  $\mathbf{A}$  and  $\mathbf{D}$  are nonsingular. Then define the  
 961 matrix function  $\mathbf{S}(\boldsymbol{\Sigma}, \mathbf{A}) = \mathbf{D} - \mathbf{C}\mathbf{A}^{-1}\mathbf{B}$  as the Schur complement of  $\boldsymbol{\Sigma}$  with respect to  $\mathbf{A}$ . Likewise,

962 there is a Schur complement with respect to  $\mathbf{D}$  by reversing the roles of  $\mathbf{A}$  and  $\mathbf{D}$ . Using Schur  
 963 complements, it is well-known (e.g, Harville, 1997, p. 97) that an inverse for a partitioned matrix  
 964  $\Sigma$  is,

$$\Sigma^{-1} = \begin{bmatrix} \mathbf{A}^{-1} + \mathbf{A}^{-1}\mathbf{B}\mathbf{S}(\Sigma, \mathbf{A})^{-1}\mathbf{C}\mathbf{A}^{-1} & -\mathbf{A}^{-1}\mathbf{B}\mathbf{S}(\Sigma, \mathbf{A})^{-1} \\ -\mathbf{S}(\Sigma, \mathbf{A})^{-1}\mathbf{C}\mathbf{A}^{-1} & \mathbf{S}(\Sigma, \mathbf{A})^{-1} \end{bmatrix}$$

965 Then, note that  $\mathbf{A}^{-1} = \mathbf{S}(\Sigma^{-1}, \mathbf{S}(\Sigma, \mathbf{A})^{-1})$ ; that is, if we already have  $\Sigma^{-1}$ , then  $\mathbf{A}^{-1}$  is the Schur  
 966 complement of  $\Sigma^{-1}$  with respect to the rows and columns that correspond to  $\mathbf{D}$ . Additionally, the  
 967 largest matrix that we have to invert is  $[\mathbf{S}(\Sigma, \mathbf{A})^{-1}]^{-1}$ , which is  $n \times n$ , which has dimension less  
 968 than  $\Sigma$ , and only one inverse is required. So, if we let  $\mathbf{A}$  correspond to the rows and columns of  
 969 the observed locations, and  $\mathbf{D}$  correspond to the rows and columns of the missing data, then this  
 970 provides a quick and efficient way to obtain  $\mathbf{V}_\rho^{-1}$  from  $\Sigma_A^{-1}$ , and the largest inverse required is  
 971  $n \times n$ , the number of missing data.

## 4 APPENDIX D: Prediction and Smoothing

Here, we give the formulas used in creating Fig. 7. For universal kriging, the formulas can be found in Cressie and Wikle (2011, p. 148),

$$\hat{y}_i = \mathbf{x}_i' \hat{\boldsymbol{\beta}} + \mathbf{c}_i \boldsymbol{\Sigma}_{-i}^{-1} (\mathbf{y}_{-i} - \mathbf{X} \hat{\boldsymbol{\beta}})$$

where  $\hat{y}_i$  is the prediction for the  $i$ th node,  $\mathbf{x}_i$  is a vector containing the covariate values for the  $i$ th node,  $\mathbf{X}$  is the design matrix for the covariates (fixed effects),  $\mathbf{c}_i$  is a vector containing the fitted covariance between the  $i$ th site and all *other* sites with observed data,  $\boldsymbol{\Sigma}$  is the fitted covariance matrix among all observed data,  $\mathbf{y}$  is a vector of observed values for the response variable, and  $\hat{\boldsymbol{\beta}} = \mathbf{X}'(\mathbf{X}'\boldsymbol{\Sigma}^{-1}\mathbf{X})^{-1}\mathbf{X}'\boldsymbol{\Sigma}^{-1}\mathbf{y}$  is the generalized least squares estimate of  $\boldsymbol{\beta}$ . The covariance values contained in  $\mathbf{c}_i$  and  $\boldsymbol{\Sigma}$  were obtained using maximum likelihood estimate for the parameters as detailed in Appendix C. We include the  $-i$  subscript on  $\boldsymbol{\Sigma}_{-i}^{-1}$  and  $\mathbf{y}_{-i}$  to indicate that, when smoothing, we predict at the  $i$ th node by removing that datum from  $\mathbf{y}$ , and by removing its corresponding rows and columns in  $\boldsymbol{\Sigma}$ . If the value is missing, then prediction proceeds using all observed values. Hence, Fig. 7a contains the observed values plus the predicted values at nodes with missing values, while Fig. 7c contains predicted values at all nodes, where any observed value at a node was removed and predicted with the rest of the observed values. The prediction standard errors are given by,

$$\hat{\text{se}}(\hat{y}_i) = \sqrt{\mathbf{c}_i' \boldsymbol{\Sigma}_{-i}^{-1} \mathbf{c}_i + \mathbf{d}_i' (\mathbf{X}_{-i}' \boldsymbol{\Sigma}_{-i}^{-1} \mathbf{X}_{-i})^{-1} \mathbf{d}_i}$$

where  $\mathbf{d}_i = \mathbf{x}_i' - \mathbf{X}_{-i}' \boldsymbol{\Sigma}_{-i}^{-1} \mathbf{c}_i$ .

For the IAR model smoothing in Fig. 7d, we used the WinBUGS (Lunn et al., 2000) software, final version 1.4.3. The model code is very compact and given below:

```

model
{
  for(i in 1:N) {
    trend[i] ~ dnorm(mu[i], prec)
    mu[i] <- beta0 + beta[stockid[i]] + b[i]
  }
  b[1:N] ~ car.normal(adj[], weights[], num[], tau)
  beta0 ~ dnorm(0, .001)
  beta[1] ~ dnorm(0, .001)
  beta[2] ~ dnorm(0, .001)
  beta[3] ~ dnorm(0, .001)
  beta[4] <- 0
  beta[5] ~ dnorm(0, .001)
  prec ~ dgamma(0.001, 0.001)
  sigmaEps <- sqrt(1/prec)
  tau ~ dgamma(0.5, 0.0005)
  sigmaZ <- sqrt(1 / tau)
}

```

991           The means of the MCMC samples from the posterior distributions of  $\mu[i]$  were used for  
 992 the IAR smoothing for the  $i$ th location in Fig. 7d.